LA-8789-T
Thesis

Restrictions on Relativistically Rotating Fluids

University of California

LOS ALAMOS SCIENTIFIC LABORATORY
Post Office Box 1663 Los Alamos, New Mexico 87545

This thesis was accepted by the University of Pittsburgh, Department of Physics and Astronomy, in partial fulfillment of the requirements for the degree of Doctor of Philosophy. It is the independent work of the author and has not been edited by the Technical Information staff.

UNITED STATES
DEPARTMENT OF ENERGY
CONTRACT W-7405-ENG. 36

Printed in the United States of America
Available from
National Technical Information Service
US Department of Commerce
5285 Port Royal Road
Springfield, VA 22161

Microfiche $3.50 (A01)

Page Range	Domestic Price	NTIS Price Code	Page Range	Domestic Price	NTIS Price Code	Page Range	Domestic Price	NTIS Price Code	Page Range	Domestic Price	NTIS Price Code
001-025	$ 5.00	A02	151-175	$11.00	A08	301-325	$17.00	A14	451-475	$23.00	A20
026-050	6.00	A03	176-200	12.00	A09	326-350	18.00	A15	476-500	24.00	A21
051-075	7.00	A04	201-225	13.00	A10	351-375	19.00	A16	501-525	25.00	A22
076-100	8.00	A05	226-250	14.00	A11	376-400	20.00	A17	526-550	26.00	A23
101-125	9.00	A06	251-275	15.00	A12	401-425	21.00	A18	551-575	27.00	A24
126-150	10.00	A07	276-300	16.00	A13	426-450	22.00	A19	576-600	28.00	A25
									601-up	†	A99

†Add $1.00 for each additional 25-page increment or portion thereof from 601 pages up.

LA-8789-T
Thesis

UC-34
Issued: March 1981

Restrictions on Relativistically Rotating Fluids

Jack R. Schendel

TABLE OF CONTENTS

ABSTRACT

A set of inequalities which apply to the surface of rigidly rotating, perfect fluids with asymptotically flat exteriors is derived. This set consists of both algebraic inequalities and inequalities which involve integrals performed over the surface of the fluid. The physical content of these inequalities is investigated by examining the restrictions they impose on the existence of rotating fluid models with Kerr interiors. For this case, the dominant set of inequalities is found and expressed in an analytic form. These restrictions impose a finite maximum redshift between observers on the surface and at infinity for all models with the Kerr parameter $a > m$. However, for all models with $0 < a/m \leq 1$, there is a unique configuration for which the redshift is unbounded. In the static limit, $a \to 0$, a finite maximum redshift depending on the matter distribution of the static background is found. This result is compared to stability requirements for non-rotating fluids. The implications of this comparison and areas for future extensions are discussed.

RESTRICTIONS ON RELATIVISTICALLY ROTATING FLUIDS

By Jack R. Schendel

1.0. INTRODUCTION

The motivation for studying rotating fluids in general relativity is two-fold. General relativity, as any other physical theory, must withstand the correspondence with observations of nature. In the case of general relativity a major testing ground comes from astronomical observations of massive objects such as compact stars and a variety of the more massive galactic nuclei. Although the physics of these objects is quite complicated and not well understood, we may gain useful insight into the gravitational interactions that take place within these objects by considering them as self-gravitating fluids as was done within the context of Newtonian gravitational theory by such researchers as Maclaurin, Jacobi, Poincare and others.

The second point of motivation arises from the first. It appears that most astrophysical objects rotate and as a consequence possess angular momentum. As in Newtonian theory, one must expect angular momentum to play a key role in applications of general relativity to astrophysical systems. These expectations are heightened when one considers the purely general relativistic effects such as frame dragging and magnetic-like interactions which occur in general relativity when the system possesses angular momentum. With this in mind, any information connecting the

behavior of material sources with the gravitational field through angular momentum could itself prove valuable in understanding angular momentum as a source of the gravitational field.

With this as motivation I now state the general mathematical requirements . I will consider two spacetime manifolds (M^+,g^+) and (M^-,g^-) which are partially bounded by a timelike hypersurface, Σ. On Σ (M^+,g^+) and (M^-,g^-) must be isometric. Hereafter, (M^+,g^+), (M^-,g^-) and Σ will be refered to as the exterior, the interior and the matching surface, respectively.

In order to simulate an isolated astrophysical system the following requirements must also be imposed on the interior and the exterior. First, the exterior must have a vanishing energy-momentum tensor and be asymptotically flat in the standard sense. In addition, the matter distribution of the interior as defined by the energy-momentum tensor T_{ab} must obey

$$T_{ab}V^aV^b \geq 0 \quad , \qquad (1.1)$$

and

$$(T_{ab}V^b)(T^{ac}V_c) \leq 0 \quad , \qquad (1.2)$$

for any timelike vector, V^a, defined on the interior manifold. The physical intepretation of eq. (1.1) is that the local matter density as measured by any observer be non-negative. Equation (1.2) requires that the local matter current as measured by any observer have a timelike flow.

1.1. Earlier Attempts

It is a very difficult problem to match rotating, physically acceptable interiors to asymptotically flat exteriors. In this section I will review some of the earlier attempts in order to illuminate some of the difficulties inherent in this problem.

1.11. Rotating Shells

One of the earliest attempts to find a solution to this matching problem came from Brill and Cohen[1], who derived an approximate solution for a slowly rotating spherical shell by considering linear perturbations of the static case. They found to first order in the angular velocity that (a) the shell is spherical and of uniform density, (b) the shell is in rigid rotation and (c) the spacetime interior is flat and all inertial frames are dragged around rigidly with the shell as the shell approaches the Schwarzschild horizon.

De La Cruz and Israel[2] attempted to extend these results to higher order. Their technique was to assume that the exterior was the Kerr solution and the interior metric could be cast in the canonical form for an axisymmetric, stationary vacuum spacetime first given by Lewis[3],

$$ds^2 = e^{2(\nu-\lambda)}(d\rho^2+ dz^2) + \rho^2 e^{-2\lambda} d\phi^2 - e^{2\lambda}(dt-\Psi d\phi)^2, \quad (1.3)$$

where ν, λ and Ψ are functions of ρ and z. In this form the field equations reduce to

$$\nu_\rho = \rho(\lambda_\rho^2 - \lambda_z^2) - (1/4)\rho^{-1} e^{2\lambda} (\Psi_\rho^2 - \Psi_z^2) \quad , \quad (1.4a)$$

$$\nu_z = 2\rho\lambda_\rho\lambda_z - (1/2)\rho^{-1}e^{4\lambda}\Psi_\rho\Psi_z \quad , \quad (1.4b)$$

$$\lambda_{\rho\rho} + \rho^{-1}\lambda_\rho + \lambda_{zz} = -(1/2)\rho^{-2}e^{4\lambda}(\Psi_\rho^2 + \Psi_z^2) \quad , \quad (1.4c)$$

and

$$\Psi_{\rho\rho} - \rho^{-1}\Psi_\rho + \Psi_{zz} = -4(\lambda_\rho\Psi_\rho + \lambda_z\Psi_z) \quad , \quad (1.4d)$$

where the subscripts denote partial differentiation. They then demand that

$$g^+_{ab}\Big|_\Sigma = g^-_{ab}\Big|_\Sigma \quad , \quad (1.5)$$

and choose a particular matching surface of the parametric form

$$\rho\Big|_\Sigma = f(\theta) \quad , \quad z\Big|_\Sigma = g(\theta) \quad . \quad (1.6)$$

Equation (1.5) fixes the functions ν, λ and Ψ on Σ. Since eqs. (1.4c) and (1.4d) form a well behaved set of elliptical partial differential equations, they arrive at a well-defined elliptical boundary value problem. Once Ψ and λ are known ν can be found via quadrature of eqs. (1.4a) and (1.4b). However, since solving eqs. (1.4c) and (1.4d) is, at best, very difficult they resort to a perturbation technique. They proceed by expanding the Kerr solution in a power series in a/R. R is the radial coordinate of the unperturbed shell and a is the Kerr angular momentum parameter. With this expansion the non-linear right sides of eqs. (1.4c) and (1.4d) are assumed known from the previous order of approximation. Thus, at each order in the approximation eqs. (1.4c) and (1.4d) become a set of linear inhomogeneous elliptical partial differential equations which can be solved by standard methods.

They then deduce the physical properties of the shell by calculating the surface stress-energy tensor which is given by

$$S_{ab} = (8\pi)^{-1} (g_{ab}\gamma - \gamma_{ab}) \quad , \quad (1.7)$$

where γ_{ab} is defined in terms of the interior and exterior extrinsic curvatures K^{+}_{ab} and K^{-}_{ab} as

$$\gamma_{ab} = K^{+}_{ab} - K^{-}_{ab} \quad , \quad (1.8)$$

and γ is the trace of γ_{ab}. The proper surface density and and the velocity u^a of the surface are then defined by

$$S_a{}^b u^a = \sigma u^b \quad , \quad (1.9)$$

where $u^a u_a = -1$. The angular velocity of the shell as measured by a stationary observer at infinity is then given by

$$\omega = \gamma^{\phi}{}_{t} / (\omega\gamma^{t}{}_{\phi} + \gamma^{t}{}_{t} - \gamma^{\phi}{}_{\phi}) \quad . \quad (1.10)$$

De La Cruz and Israel carried out this procedure to third order in the Kerr parameter and found that, to first order, the results of Cohen and Brill were reproduced exactly. However, in the third order of the approximation these results break down. They showed that in no case could the shell be uniform and simultaneously be in rigid rotation. They did find that the interior inertial frames were dragged with the shell as the matching surface approached the outer Kerr horizon. However, the credibility of the interpretation of the model in this limit is somewhat strained by the fact that the surface stresses become infinite in this limit. Because of these results and the

complicated nature of higher orders they conclude that a rotating shell does not appear to be the natural source of the Kerr solution.

1.12. Rotating Disks: The Model of Bardeen and Wagoner

Bardeen and Wagoner[4,5] have constructed and explored a sequence of rotating disk models. They assume that the matter is a perfect fluid in rigid rotation and confined to a disk perpendicular to the axis of rotation. In order to simplify the field equations they ignore the pressure and, in particular, its effects on the structure perpendicular to the disk. In doing so, the interior matter distribution takes on the form of boundary conditions imposed on the exterior .

They begin by choosing two parameters necessary to specify their model. Instead of the mass and angular momentum, they choose the coordinate radius of the disk, which sets the basic scale of the model, and a parameter γ which is related to the integral of the equation of hydrostatic support such that

$$\gamma = z_c/(z_c + 1) \quad , \quad (1.11)$$

where z_c is the redshift at the center of the disk. The parameter γ varies from zero in the Newtonian limit to one in the extreme relativistic limit. They proceed by expanding a variant of the canonical axisymmetric, stationary metric eq. (1.3) and the resulting field equations equivalent to eqs. (1.4) in a power series in γ. As in the case of De La Cruz and Israel, Bardeen and Wagoner's

versions of eqs. (1.4) become inhomogeneous but linear partial differential equations with the inhomogeneous terms being known from lower orders of the approximation. Further simplification arises when it is noted that in oblate spheroidal coordinates their versions of eqs. (1.4c) and (1.4d) are separable yielding ordinary differential equations at each order of the approximation. Once these equations are solved at a particular order, then their version of ν can be found via quadrature of eqs. (1.4a) and (1.4b).

Boundary conditions at the disk are imposed in the form of self-consistency requirements on the surface density which is defined in a manner analogous to that of De La Cruz and Israel. They require that the equation of hydrostatic support be satisfied parallel to the disk and that the surface density be positive and also finite at the rim of the disk. In addition, they demand asymptotic flatness.

The equations are then solved analytically through the post-Newtonian order. Beyond this order the equations are integrated numerically using the analytic results through the second order in γ as starting points. The numerical calculations are carried out independently by both Bardeen and Wagoner through fifth order. Bardeen continues the calculation through tenth order where he estimates the accuracy to be better than one per cent, even in the extreme relativistic limit. These estimates are based on analytic asymptotic relations between the functions Ψ and λ and the mass and angular momentum.

This method of calculation yields a sequence of equilibrium models. The physical interpretation of this sequence is that a disk of fixed rest mass (as defined by the surface density) loses angular momentum, contracts and becomes more relativistic as γ approaches one. In this sequence the angular momentum monotonically decreases to a finite value in the extreme relativistic limit. They also note that the binding energy, defined as the difference between the rest mass and the gravitational mass, is positive and increases monotonically with γ indicating that these models become more stable to gravitational collapse as they become increasingly relativistic. For $\gamma \leq 1/2$ the maximum surface density occurs at the center and decreases to zero at the rim. For $\gamma \geq 1/2$ the maximum of the density occurs away from the center. In the relativistic limit the mass tends to be concentrated near the rim in a somewhat ring-like distribution.

By examining the angular velocity and the geometry of the exterior, Bardeen and Wagoner conjecture that in the extreme relativistic limit the geometry of the exterior becomes that of the extreme Kerr geometry (that is, $a = m$). The angular velocity of the disk as measured by a stationary observer at infinity approaches the angular velocity of the outer horizon of the extreme Kerr geometry in this limit. They also calculate the quadrupole moment as defined by the asymptotic structure of their exterior geometry and find that in this limit the ratio of the quadrupole moment to the

to the monopole moment is one as in the case of the extreme Kerr geometry. One more fact supports their conjecture. At $\gamma \approx 0.6$ an ergotoroid forms near the rim and as γ approaches one it approaches the ergosphere of the extreme Kerr geometry.

Although these results are suggestive that the exterior geometry of a rotating disk approaches the extreme Kerr geometry in the relativistic limit, there are some problems. Bardeen and Wagoner admit that their technique loses accuracy near the disk in this limit. They also note that there are two distinct instabilities inherent in this problem. The first is that thin disks are highly unstable to fragmentation. Although a fully relativistic treatment of this instability is not done, fragmentation instabilities in the Newtonian regime will probably carry over due to the fact that they ignore all structure perpendicular to the disk by considering it to be infinitesimally thin. The second instability arises from the appearance of marginally trapped surfaces in the extreme relativistic limit. As they argue, any perturbation will lead to a genuinely trapped surface and eventually to a singularity. These problems lead to the conclusion that the limiting case of γ approaching one is not physically realizable.

1.13. Slowly Rotating Spheroids: The Model of Chandrasekhar and Miller

Chandrasekhar and Miller[6] have constructed slowly rotating constant density models. Their approach is

different from either of the models discussed above. Following a technique developed by Hartle and Thorne[7] they perturb away from a fully relativistic, static, spherically symmetric solution of the field equations in an attempt to understand the effects of slow rotation in the relativistic regime.

Hartle and Thorne developed their technique to study relativistic models of neutron stars. The algorithm is as follows. They choose a realistic equation of state and then numerically construct a fully relativistic, static ,spherically symmetric, perfect fluid model. They then expand the metric, the mass density, and the pressure in a power series in the angular velocity to second order. The perturbation from spherical symmetry arises from second order terms which they assume contain quadrupole-like terms. The resulting equations are solved numerically and they find that the surface becomes deformed due to the quadrupole perturbations in the pressure.

Chandrasekhar and Miller choose an incompressible homogeneous fluid as opposed to the more realistic equations of state of Hartle and Thorne for two reasons. The first reason is that an analytic, static, spherically symmetric solution of the field equations is known for this equation of state. This is the well-known interior Schwarzschild solution. The second and more important reason is that relativistic effects are more easily studied with such a model since this model is more compact than the numerical neutron

star models of Hartle and Thorne. For incompressible homogeneous perfect fluids, stable configurations exist for radii down to nine-eighths of the Schwarzschild radius. At this point the pressure becomes unbounded . This is a special case of the results of Buchdahl[8] and Bondi[9] concerning limiting surface redshifts for more general equations of state. Hartle and Thorne find that for their equations of state stable models do not exist for radii less than two and one-half times the Schwarzschild radius. Thus, relativistic effects are better explored with less realistic equations of state.

Based on their numerical calculations, Chandrasekhar and Miller find the following results. In the relativistic limit (i.e.,as $R \to 9/8\ R_s$) the quadrupole moment becomes very close to that given by the Kerr exterior. They also find that an ergoregion seems to form in this relativistic limit. From these results they speculate that the relativistic limit of their model seems to be matched to a Kerr exterior.

They also calculate the eccentricity of isobaric surfaces and find that as R decreases the eccentricity begins to diverge in the relativistic limit indicating the relativistic limit will approach a disk-like configuration. However at $R \approx 2.4\ R_s$ the eccentricity falls drastically. From this evidence they question the existence of disk-like configurations within general relativity.

1.14. Some Purely Numerical Attempts

Bonnazzola and Schneider[10] have numerically integrated the field equations for a rigidly rotating perfect fluid with a degenerate Fermi gas equation of state. They conclude on the basis of their calculated quadrupole moment that it may be possible to match their model to a Kerr exterior. However, they find that the inner isobaric surfaces are prolate rather than oblate as might be expected from the work of Chandrasekhar and Miller who find that these surfaces become spherical in the relativistic limit of their model.

Butterworth and Ipser[11,12] argue that the method of Bonnazzola and Schneider incorporates artificial restrictions which preclude relativistic effects such as the formation of ergoregions. This is done by discarding solutions that may be associated with coordinate singularities. They proceed to numerically integrate the field equations and find some interesting results. They find that ergoregions do form. They also find that sequences of rigidly rotating homogeneous models of increasing eccentricity terminate at a maximum eccentricity. Their physical explanation is that at this point mass begins to shed at the equator. This appears to be a somewhat unexpected general relativistic result as Maclaurin spheroids do not exhibit this behavior although post-Newtonian corrections to the Maclaurin sequence do imply this behavior. These results, like those of Chandrasekhar and Miller, seem to preclude disk-like configurations.

1.2. A Different Approach

In the previous section I have reviewed some of the previous attempts to understand rotating fluids in general relativity in order to illuminate some of the difficulties inherent to the problem of constructing fluid models. In reviewing these attempts one also gains an appreciation for the approximate and somewhat tenuous nature of the results. With this in mind, the approach taken here will be quite different. Rather than attempting to solve the field equations either exactly or approximately for a particular model, I will seek general restrictions on rotating fluids arising from the full field equations.

In order to have some chance of succeeding in this undertaking, I will restrict this study to stationary, axisymmetric, rigidly rotating perfect fluids. Roos[13] has shown that for rotating fluids with an analytic equation of state solutions exist within the neighborhood of the matching surface provided that the surface is tangent to both the timelike and rotational Killing vectors. Although there is no guarantee that such solutions exist globally, these solutions cannot be completely excluded by any known local arguments.

There is an argument against the stationarity of such solutions due to Friedman and Schutz[14,15]. They argue that all rotating perfect fluids are dynamically unstable due to the emission of gravitational radiation. The generic instability they describe is motion to lower energy con-

figurations via bar-like perturbations. Purely Newtonian stars are stable to such perturbations. However, they show that within general relativity these bar like perturbations give rise to gravitational radiation which further drives these perturbations by carrying off angular momentum. This is consistent with Chandrasekhar's investigation[16] of the effects of gravitational radiation reaction on the sequence of Maclaurin spheroids. He finds that the introduction of this reaction force causes the Maclaurin sequence to branch off onto the sequence of Dedekind ellipsoids which have lower angular momentum. Although this instability does indicate that a rotating star can not be described by a globally stationary solution to the field equations, loose estimates based on Chandrasekhar's work indicate that the time scale for the growth of these instabilities may be much longer than the age of the universe for main sequence stars. From this fact, it seems reasonable, although not entirely correct, to model rotating stars as globally stationary solutions of the field equations.

In chapter two I will define the basic mathematical properties of the physical systems to which this study will be restricted. After these definitions the field equations will be explored and found to demand that certain algebraic and integral inequalities be satisfied. The physical interpretation of these inequalities will also be discussed. In chapter three these general results will be applied to an interior matched to a Kerr exterior. A

combination of the inequalities is found to give rise to a very simple result: There exists for each Kerr exterior for which $a \leq m$ only one possible extreme relativistic configuration characterized by its angular velocity which is identical to the angular velocity associated with the horizon of the Kerr black hole. In chapter four this result and its implications will be discussed. Areas for future extensions of this work will also be considered.

2.0. STATIONARY, AXISYMMETRIC PERFECT FLUIDS

2.1. Preliminary Definitions

In this section I will define a possible class of rotating fluid solutions of the field equations. This class consists of stationary, axisymmetric perfect fluids undergoing rigid rotation. Although some of the results presented here can be extended to the case of differential rotation, only the case of rigid rotation will be considered here.

The following conventions will be employed throughout the remainder of this work. The physical spacetime will be assumed to have the signature of (-,+,+,+). Small latin indices will be used to label components of tensors on the spacetime and will run from 0 to 3. Geometrized units where G=c=1 will be used.

2.11. Stationary, Axisymmetric Spacetimes

By stationary one normally means that the system under study maintains the same behavior at all times. More precisely, stationarity implies the existence of a one parameter group of transformations which maps earlier events into later events. I shall adopt as the definition of stationarity Carter's definition of pseudo-stationarity[17]: A spacetime is pseudo-stationary if it is invariant under the the action of a continuous one-parameter group of isometries which is generated by a Killing vector field, ξ_0^m, which is timelike at least asymptotically. The demand of asymptotic

flatness, which is taken here to mean Newtonian behavior far from the fluid, allows the normalization

$$\xi_0^m \, \xi_{0m} \to -1 \qquad (2.1)$$

at infinity.

The existence of this timelike Killing vector field gives rise to a conserved quantity, the total mass, m, which can be used to characterize the spacetime. This mass, as defined by Komar[18], is expressed in terms of an integral over a closed two surface at infinity as

$$m \equiv -(1/8\pi) \oint \nabla^{[a} \xi_0^{b]} dS_{ab} \quad , \qquad (2.2)$$

where the square brackets denote the standard antisymmetrization of indices.

Axisymmetric normally implies that there is a preferred curve called the axis of rotation which serves as the center of rotations that leave the system unchanged. I shall use the following as a definition: A spacetime is axisymmetric if it is invariant under a continuous one parameter group of isometries which is generated by a Killing vector field, ξ_1^m, whose integral curves are diffeomorphic to circles and which is globally defined to be spacelike except on the axis of rotation where it vanishes identically. Here, the axis of rotation is a timelike two surface. The condition that the integral curves of ξ_1^m be diffeomorphic to circles means that these integral curves defined by

$$\frac{dx^a}{d\phi} = \xi_1^a \qquad (2.3)$$

must describe closed rotational orbits for the parameter range, $0 \leq \phi \leq 2\pi$ to eliminate the possibility of pseudo-rotations.

As in the case of stationary spacetimes, the existence of this rotational Killing vector field gives rise to a conserved quantity, the angular momentum J, which characterizes the spacetime. Again following Komar[18], the angular momentum of the spacetime is defined to be

$$J \equiv (1/16\pi)\oint \nabla^{[a}\xi_{1}^{b]} dS_{ab} \quad , \tag{2.4}$$

where the integral is performed over a closed two-surface at infinity.

From the above definition, it is clear that the group of isometries generated by ξ_{1}^{m} is isomorphic to the ordinary one-parameter rotation group. The group of isometries generated by ξ_{0}^{m} is isomorphic to R(1), the group of translations on the real line. When a spacetime is stationary and axisymmetric the two Killing vector fields together generate a two-parameter abelian group formed as the direct product R(1)XSO(2). Carter[19] has shown that this direct product structure implies that the two generators commute.

2.12. Perfect Fluids

In general, fluids can be quite complicated due to the vast number of microscopic interactions which are incorporated in the macroscopic theory of fluids. Within general relativity, all of these interactions, in principle, must be included in the energy-momentum tensor. A vast

simplification arises by describing the energy-momentum tensor of the fluid in macroscopic variables and ignoring their microscopic origins. However, the energy-momentum tensor of a real fluid with isotropic pressure and no electromagnetic charge is still quite complicated and is given by[20]

$$T^{ab} = \mu u^a u^b + (p-\zeta\theta)P^{ab} - 2\eta\sigma^{ab} + q^{(a}u^{b)} , \qquad (2.5)$$

where the parenthesis indicate standard symmetrization of indices, μ is the mass density, p is the pressure, ζ and η are the bulk and dynamic coefficients of viscosity, u^a is the four velocity field of the fluid, θ, σ^{ab} and P^{ab} are, respectively, the expansion, the shear tensor and the projection tensor of u^a and q^a is the heat flow vector. The heat flow vector can be expressed in terms of the temperature field of the fluid, T, and the thermal conductivity, κ, of the fluid as

$$q^a = -\kappa P^{ab}(\nabla_b T + T a_b) , \qquad (2.6)$$

where a_b is the acceleration of the flow and ∇_b is the covariant derivative of the spacetime.

It is obvious from the above definition that the problem of solving Einstein's equations,

$$G^{ab} = 8\pi T^{ab} , \qquad (2.7)$$

and the equations of motion,

$$\nabla_b T^{ab} = 0 , \qquad (2.8)$$

including viscous effects and heat flows very quickly becomes unmanageable. Since the intent here is to isolate the effects of angular momentum, I shall restrict this study to non-viscous fluids having no thermal conductivity, hereafter referred to as perfect fluids. With this definition, the energy-momentum tensor for a perfect fluid becomes

$$T^{ab} = (\mu + p)\, u^a\, u^b + p\, g^{ab} \quad , \tag{2.9}$$

where g^{ab} is the metric of the spacetime.

With this definition of a perfect fluid, the energy conditions, eqs. (1.1) and (1.2), reduce to

$$|p| \leq \mu \quad . \tag{2.10}$$

This condition must be imposed on the equation of state which is taken here to mean a functional relation between μ and p, $\mu = \mu(p)$. An additional requirement will also be imposed on the equation of state: the pressure vanishes when the mass density vanishes. This requirement allows the matching surface to be defined as the surface on which the pressure vanishes as is the normal procedure in Newtonian stellar structure.

A restriction stronger than the energy condition, eq. (2.10), will also be imposed on the fluid. The pressure will always be assumed to be positive near the matching surface. Although there are no a priori reasons to reject negative pressure, it is highly unlikely that materials exhibiting characteristics of negative pressure are stable to gravitational collapse. Thus, it would be unreasonable to expect such systems to be stationary.

2.13. Classes of Fluid Flows

Although fluid flows, in general, can be quite complicated, they can be quite simply classified for spacetimes which are stationary and axisymmetric. A fluid flow is defined to be circular or purely rotational if the four velocity field of the fluid is a linear combination of the two independent Killing vector fields; i.e.,

$$u^a = (-\Psi)^{-1/2} \left(\underset{0}{\xi}{}^a + \Omega \underset{1}{\xi}{}^a \right) \quad , \qquad (2.11)$$

where the factor containing the Ψ is defined as the redshift factor and insures that

$$u^a \underset{a}{u} = -1 \quad . \qquad (2.12)$$

Because of the timelike character of u^a, Ψ must be negative. Ω in eq.(2.11) defines the angular velocity of the fluid. Two distinct subclasses of circular flows are defined by the behavior of Ω. If Ω is constant the fluid is said to be in rigid rotation. If Ω is not constant the fluid is said to be in differential rotation. By convention, Ω will always be taken to be positive.

The second class of fluid flows is non-circular flows. This motion is characterized by the property that the velocity field of the fluid is orthogonal to the rotational Killing vector field,

$$\underset{1}{\xi}{}^m \underset{m}{u} = 0 \quad . \qquad (2.13)$$

Two distinct subclasses of non-circular flows exist, convective flows and what I shall call radial flows. The

distinction between these two subclasses is that the projection of the integral curves of the velocity onto a purely spacelike hypersurface is closed for convective flows and is not closed for radial flows. Radial flows could be used to model the gravitational collapse of a star which has exhausted its nuclear fuel or, perhaps, the explosive process of a star becoming a supernova. Convective flows are defined in such a way that they model the normal process of convection which occurs in main sequence stars.

As the motivation of this study is to explore the role that angular momentum plays in general relativistic astrophysical systems, of all the classes of flows purely rotational flows must be the most important. This is not to say that a general relativistic treatment of convective flows would not be of interest. It is simply beyond the scope of this study. It should also be obvious that the use of radial flows which are strictly stationary to model the above-mentioned catastrophic stellar phenomena offers little hope. For these reasons I shall restrict this study to purely rotational flows as defined by eq. (2.11). In addition, only rigid rotations will be considered here due to the added complexity which arises from differential rotation.

2.2. Reduction of the Field Equations

Geroch[21] has developed a formalism which allows the field equations to be simplified in a covariant manner when the spacetime admits two commuting Killing vector fields. His reduction is obtained by mapping the physical spacetime M and the physical fields defined on M to the manifold of trajectories of the Killing vector fields, S. Each point in S corresponds to a particular orbit of the Killing vector fields in M. Two points in M are mapped into the same point in S if they can be connected by a curve in M whose tangent is everywhere a linear combination of the two commuting Killing vector fields.

As it will be used here, this mapping is isomorphic to a projection of the physical spacetime M onto a two-dimensional surface everywhere orthogonal to the two Killing vector fields. The existence of such a surface is not guaranteed in general. Because ξ_0^m and ξ_1^m commute, there does exist a family of two-surfaces which are everywhere tangent to ξ_0^m and ξ_1^m. These surfaces are known as surfaces of transitivity. If the spacetime also possesses a family of two-surfaces orthogonal to ξ_0^m and ξ_1^m the spacetime is said to be orthogonally transitive. It can be shown that the conditions for a spacetime to be convection-free are equivalent to the conditions that the spacetime be orthogonally transitive. Thus, with the assumption of circular flow the existence of the two-dimensional surface described above is guaranteed.

2.21. Reduction for Perfect Fluids

Hansen and Winicour[22] have applied the Geroch formalism to spacetimes which have a non-vanishing matter distribution described by the energy-momentum tensor of a perfect fluid. They begin with a spacetime M which admits a pair of commuting Killing vector fields, ξ^m_0 and ξ^m_1, such that they are everywhere timelike and spacelike respectively. It is convenient to write the pair (ξ^m_0, ξ^m_1) as ξ^m_A, where A runs from 0 to 1 as will all other upper case latin indices. These additional indices are not merely for convenience but represent a hidden symmetry of the field equations. This hidden symmetry has been reviewed by Kinnersley[23]. The basis of this symmetry is that the field equations are invariant under the action of a group of transformations which replace ξ^m_0 and ξ^m_1 by linear combinations of themselves. This group of transformations is isomorphic to SO(2,1) and manifests itself as a gauge freedom in the way the Killing scalars, defined as

$$\lambda_{00} \equiv \xi^m_0 \, \xi_{0m} \quad , \qquad (2.14a)$$

$$\lambda_{01} \equiv \xi^m_0 \, \xi_{1m} \quad , \qquad (2.14b)$$

and

$$\lambda_{11} \equiv \xi^m_1 \, \xi_{1m} \qquad (2.14c)$$

transform under the action of the group. One finds that the

triad defined as

$$\lambda_{\mu} \equiv (\lambda_{00}, \lambda_{01}, \lambda_{11}) \quad , \qquad (2.15)$$

transforms as a vector under the action of SO(2,1) with a norm given by

$$G^{\mu\nu} \lambda_{\mu} \lambda_{\nu} \equiv 2(\lambda_{00} \lambda_{11} - \lambda_{01}^{2}) \quad , \qquad (2.16)$$

where $G^{\mu\nu}$,a constant scalar field on S, is the metric of the SO(2,1) vector space. The function τ^2 defined as

$$\tau^{2} \equiv - G^{\mu\nu} \lambda_{\mu} \lambda_{\nu} \quad , \qquad (2.17)$$

is a positive scalar field on S . Hereafter, lower case greek indices refer to the transformation properties of the object with respect to SO(2,1) and range from one to three.

The metric, h_{ab} , on S is given by

$$h_{ab} = g_{ab} + 2 \tau^{-2} \lambda^{MN} \xi_{Ma} \xi_{Nb} \quad , \qquad (2.18)$$

and is used to project tensor fields defined on M onto S. The indices of tensors on S run from zero to three. However, only the components orthognal to ξ^{m}_{0} and ξ^{m}_{1} are non-zero (i.e., by choosing a coordinate system in which $\xi^{m}_{0} = \delta^{m}_{0}$ and $\xi^{m}_{1} = \delta^{m}_{3}$ the indices of the non-zero components of tensors on S run from one to two). The alternating tensor on S is given by

$$\varepsilon_{ab} = (\sqrt{2} \tau)^{-1} \varepsilon^{MN} \varepsilon_{abmn} \xi^{m}_{M} \xi^{n}_{N} \quad , \qquad (2.19)$$

where ε_{abmn} is the alternating tensor of M and ε_{MN} is the alternating symbol defined by the rules

$$\varepsilon^{AM}\,\varepsilon_{MB} = \delta^{A}_{\ B} \quad , \qquad (2.20a)$$

$$x^{A} = \varepsilon^{AB}\,x_{B} \quad , \qquad (2.20b)$$

and

$$x_{A} = \varepsilon_{AB}\,x^{B} \qquad (2.20c)$$

for any object x and which is used to raise and lower upper case latin indices. ε_{AB} is related to $G_{\alpha\beta}$ in the following way,

$$G_{\alpha\beta} = -\,\varepsilon_{A(C}\,\varepsilon_{D)B} \quad , \qquad (2.21)$$

where the index α is identified with the pair (AB) and β is identified with the pair (CD).

The covariant derivative D_a on S of a tensor field $Q^{a\ldots b}_{\ \ c\ldots d}$ defined on S is given by

$$D_a Q^{b\ldots c}_{\ \ d\ldots e} = h^{m}_{\ a}\,h^{b}_{\ n}\ldots h^{c}_{\ p}\,h^{r}_{\ d}\ldots h^{s}_{\ e}\,\nabla_m\,Q^{n\ldots p}_{\ \ r\ldots s} \quad , \qquad (2.22)$$

where ∇_a is the covariant derivative on M. The Riemann tensor $\mathcal{R}^{a}_{\ bcd}$ of S is defined by

$$D_{[a}\,D_{b]}\,k_{c} = (1/2)\,\mathcal{R}_{abc}^{\ \ \ m}\,k_{m} \quad , \qquad (2.23)$$

where k_a is any vector field defined on S.

In general to proceed with the reduction one is

required to define two additional scalar fields on S given by

$$c_A = (1/2)\,\epsilon^{MN}\,\epsilon^{mnpq}\,\xi_{Mm}\,\xi_{Nn}\,\nabla_p\,\xi_{Aq} \quad . \qquad (2.24)$$

These two fields measure the circulation of the spacetime. With the assumption of purely rotational flow, these fields vanish. With this fact the procedure of projecting the field equations onto S yields

$$D^m(\tau^{-1}D_m\lambda_\mu) = \tau^{-3}\lambda_\mu\,(D^m\lambda^\nu)(D_m\lambda_\nu) - 2\tau^{-1}R_{mn}\,\xi^m_A\,\xi^n_B \quad , \qquad (2.25)$$

$$\mathcal{R}_{ab} = (1/2)\tau^{-2}\,(D_a\lambda^\mu)(D_b\lambda_\mu) + \tau^{-1}D_aD_b\tau + h^m_a h^n_b R_{mn} \quad , \qquad (2.26)$$

$$D^m(\tau\,h^n_m R_{mp}\,\xi^p_A) = 0 \quad , \qquad (2.27)$$

and

$$D^m\,[\tau(h^n_a h^p_m R_{np} - (1/2)h_{am}h^{np}R_{np})]$$

$$= -(1/2)h^{mn}R_{mn}D_a\tau - \tau^{-1}\lambda^{MN}D_a(R_{mn}\,\xi^m_M\,\xi^n_N) \quad , \qquad (2.28)$$

where R_{mn} is the Ricci tensor of M. These last two equations arise from the Bianchi identities.

Up to this point no particular source has been chosen and eqs. (2.24) through (2.28) describe a general convection-free spacetime with two commuting Killing vector fields. The specific source can now be added through the full field equations on M,

$$R_{mn} = 8\pi(T_{mn} - (1/2)T\,g_{mn}) \quad . \qquad (2.29)$$

By defining $s^M \equiv (1,\Omega)$ the velocity field, assumed to be

purely rotational takes the form

$$u^a = (-\Psi)^{-1/2}\ s^M\ \underset{M}{\xi}{}^a \quad . \tag{2.30}$$

In order to compactify the notation, it is useful to define the SO(2,1) vector

$$S^\mu \equiv s^M\ s^N = (1, \Omega, \Omega^2) \quad , \tag{2.31}$$

which is related to Ψ by

$$\Psi = S^\mu\ \underset{\mu}{\lambda} = \underset{00}{\lambda} + 2\ \Omega\ \underset{01}{\lambda} + \Omega^2\ \underset{11}{\lambda} \tag{2.32}$$

due to the unit norm of the velocity. With this notation the field equations for a stationary, axisymmetric rigidly rotating perfect fluid take the compact form

$$D^m[\tau^{-1} D_m \underset{\mu}{\lambda}] = \tau^{-3}\ \underset{\mu}{\lambda}\ (D^a \underset{\beta}{\lambda})(D_a \lambda^\beta)$$

$$+ 8\pi\tau^{-3}[(\mu+3p)\underset{\mu}{\lambda} + (\mu+p)\tau^2\ \Psi^{-1} S_\mu] \quad , \tag{2.33}$$

$$\mathcal{R} = (1/2)\tau^{-2}(D^m \underset{\mu}{\lambda})(D_m \lambda^\mu) + 8\pi(\mu+p) \quad , \tag{2.34}$$

and

$$(\mu+p)\Psi^{-1}\ D_a \Psi = -2\ D_a p \quad . \tag{2.35}$$

Equations (2.33) and (2.34) are the projections of the field equations onto S and determine the variables $\underset{ab}{h}$ and $\underset{\mu}{\lambda}$. Equation (2.35) is the result of projecting the Bianchi indentities and, therefore, is an integrability condition imposed on the solutions of eqs. (2.33) and (2.34). A solution of these equations specified by $\underset{ab}{\bar{h}}$, $\underset{\mu}{\lambda}$, μ and p are equivalent to a solution of the field equations specified by

g_{ab}, u^a, μ and p on the physical spacetime. This can be seen by using the coordinate freedom to choose $\xi^m_0 = (1,0,0,0)$ and $\xi^m_1 = (0,0,0,1)$ which cooresponds to a coordinate system in which the coordinates x^0 and x^3 parameterize the integral curves of the timelike and rotational Killing vector fields respectively. This choice determines the metric of the physical spacetime, g_{ab}, in terms of h_{ab} and λ_μ via eqs. (2.17) and (2.18). The velocity field u^a is determined by the Killing vector fields and λ_μ via eqs. (2.30) and (2.32).

2.22. Extension to the Manifold of Trajectories with Boundary

A problem arises due to the fact that the rotational Killing vector vanishes on the axis of rotation. At these points in M the mapping from M to S becomes singular leaving S topologically equivalent to a half-plane which is without boundary on the left side. Hansen and Winicour[22,24] have extended the manifold of trajectories, S, to the manifold of trajectories with boundary, $\tilde{S}$, by imposing regularity conditions on the points on the axis of rotation.

The following conditions are imposed to guarantee the regularity of the points on the axis:

$$\tau = \lambda_{01} = \lambda_{11} = n^m D_m \lambda_\alpha = 0 \qquad ,(2.36a)$$

$$a \equiv n^m D_m \tau > 0 \qquad ,(2.36b)$$

and

$$b \equiv n^m D_m (n^p D_p \lambda_{11}) > 0 \qquad , (2.36c)$$

where n^m is the unit normal to the axis and a and b are

smooth functions along the axis. The vanishing of τ, λ_{01}, and λ_{11} follows from the fact that ξ^m_1 vanishes on the axis. The vanishing of the normal derivative of λ_α is imposed to prevent discontinuities in its derivative in M which would give rise to singularities in M. Eq. (2.36b) sets the sign τ in S, as the definition of τ, eq. (2.17), allows τ to be either positive or negative. Eq. (2.36c) precludes the possibility of conical singularities forming on the axis.

With the above regularity conditions the compactification of S is performed by adding the points on the axis, yielding the manifold of trajectories with boundary $\tilde{S}$. Hereafter, references to the manifold of trajectories will mean $\tilde{S}$ and the tildes will be dropped.

2.3. Generalizations of Two Newtonian Results

In this section fully relativistic generalizations of Von Zeipel's theorem and the Newtonian virial theorem will be exhibited. The first generalization can be stated as: The surfaces of constant density, the isobaric surfaces and the surfaces of constant redshift coincide. Boyer[25] first recognized that the conservation of energy and momentum eq. (2.35) implies that the isobaric surfaces and the surfaces of constant redshift must coincide. Since the redshift between two stationary observers, one on the surface and one at infinity can be expressed as

$$z = (-\Psi)^{-1/2} - 1 \quad , \qquad (2.37)$$

surfaces of constant Ψ are surfaces of constant redshift. These surfaces must coincide with isobaric surfaces since the gradients of p and Ψ are antiparallel. By writing eq. (2.35) as

$$D_m(\ln\Psi) + 2(\mu+p)^{-1}D_m p = 0 \quad , \quad (2.38)$$

and then taking the curl of this equation,

$$\varepsilon^{anm} D_n[D_m(\ln\Psi) + 2(\mu+p)^{-1}D_m p] = 0 \quad , \quad (2.39)$$

one finds that

$$\varepsilon^{amn} (D_m\mu)(D_n p) = 0 \quad , \quad (2.40)$$

which implies that the gradients of μ and p are parallel. Thus, it follows that the isobaric surfaces and the surfaces of constant density must coincide.

The surfaces of constant redshift become the "level" surfaces of Newtonian theory. These are surfaces where the difference between the gravitational potential energy and the kinetic energy is a constant, which can be seen by examining the Newtonian limit of Ψ = const . In this limit the timelike and rotational Killing vector fields become $\partial/\partial t$ and $\partial/\partial\phi$ respectively, where t is the Newtonian time and ϕ is the azimuthal angle of a circular cylindrical coordinate system. In coordinates (t,ρ,ϕ,z) the components of the Killing vector fields are $\xi^m_0 = \delta^m_0$ and $\xi^m_1 = \delta^m_2$. This implies that in the Newtonian limit

$$\lambda_{00} = g_{00} \to -1 - 2\phi \quad , \quad (2.42a)$$

$$\lambda_{01} = g_{02} \to 0 \quad , \quad (2.42b)$$

$$\lambda_{11} = g_{22} \to \rho^2 \quad , \quad (2.42c)$$

where ϕ is the Newtonian gravitational potential and ρ is the distance from the axis in the Newtonian limit. Thus, in the Newtonian limit Ψ = constant becomes

$$-\phi + (1/2)\Omega^2\rho^2 = \text{const} \quad , \quad (2.43)$$

and Von Zeipel's theorem is recovered exactly: Level surfaces coincide with the isobaric surfaces.

The conservation of energy and momentum, eq. (2.35), can be used to produce other results. Taking the inner product of this equation with n^m, the outward directed normal to an isobaric surface, yields

$$n^m D_m \Psi = -2\Psi(\mu+p)^{-1} n^m D_m p \quad . \quad (2.44)$$

If the isobaric surface is chosen to be the matching surface where the pressure vanishes, one finds that

$$n^m D_m \Psi \leq 0 \quad , \quad (2.45)$$

due to the fact that Ψ is negative to insure the timelike flow of the fluid, μ and p are positive and the gradient of p must be directed inward.

Given an equation of state, $\mu = \mu(p)$, one can integrate eq. (2.44) inward from the matching surface. This yields

$$\Psi = \Psi_\circ \exp\left[-2 \int_0^p (\mu+p)^{-1} dp\right] \quad , \quad (2.46)$$

where $\Psi_\circ$ is the quantity which determines the redshift of the matching surface. This equation allows $\Psi_\circ$ to be chosen

as one of the interior parameters. Normally the central density or the central pressure is used to parameterize either Newtonian or relativistic stellar models; however, neither of these quantities will be known without detailed knowledge of the interior. Since Ψ_o is related to the central density via eq. (2.46) and the equation of state it will be used to parameterize the interior together with the angular velocity Ω.

A second relativistic generalization of a Newtonian result which can be found is the virial theorem. This theorem follows from the definition of the total mass and the angular momentum of the spacetime, eqs. (2.2) and (2.4). These integrals can be expressed in terms of volume integrals involving the energy-momentum tensor by using the Gauss theorem and the field equations. The results are

$$m \equiv -2 \int_0 \xi^a \left[T_a{}^b - (1/2)\, \delta_a{}^b\, T \right] dS_b \qquad ,(2.47)$$

and

$$J \equiv \int_1 \xi^a\, T_a{}^b\, dS_b \qquad ,(2.48)$$

where the integration is performed over the interior and dS_a is chosen such that

$$\xi^a_1\, dS_a = 0 \qquad ,(2.49)$$

Equations (2.48) and (2.49) can be written in terms of the Killing scalars as

$$m = -2 \int \left[\mu + 3p - 2\Omega(\mu+p)\Psi^{-1}\eta \right] \xi^a_0\, dS_a \qquad ,(2.50)$$

and

$$J = \int \left[(\mu+p)\Psi^{-1}\eta \right] \xi^a_0\, dS_a \qquad ,(2.51)$$

where η is a linear combination of the Killing scalars defined by the SO(2,1) vector $N^{\alpha} = (0,1,\Omega)$ as

$$\eta \equiv N^{\alpha} \lambda_{\alpha} = \lambda_{01} + \Omega \lambda_{11} \quad .(2.52)$$

By combining eqs.(2.50) and (2.51) one finds that

$$m = 2\Omega J + \int_{0} (\mu+3p)\xi^{a} \, dS_{a} \quad . (2.53)$$

As shown by Abramowicz, Lasota and Muchotrzeb[26], in the Newtonian limit this becomes

$$E_{grav} + 2 E_{rot} + 3 \int_{I} pdV = 0 \quad , (2.54)$$

where E_{grav} is the Newtonian gravitational energy, E_{rot} is the Newtonian rotational energy and the pressure integral is performed over the volume of the fluid I.

It should be noted that with the assumptions of positive pressure and matter density eq. (2.53) imposes the following condition on m, J and Ω

$$m \geq 2\Omega J \quad . (2.55)$$

This restriction, hereafter referred to as the virial theorem, is the first explicit restriction involving only the parameters needed to describe the system.

2.4. The Algebraic Inequalities of Hansen and Winicour

Hansen and Winicour [22,24] have used the structure of the field equations coupled to boundary conditions to prove certain inequalities, among which is the positivity of the angular momentum density. In examining the integrand of

eq. (2.51) it is seen that the sign of the angular momentum density is determined by the sign of η. This is because Ψ is negative and the quantity $\mu+p$ is positive.

In this and later calculations, the following combination of the field equations, eq. (2.33), will prove useful:

$$A^{[\gamma}B^{\nu]}D^{m}[\tau^{-1}\lambda_{\nu}\ D_{m}\lambda_{\gamma}] = 8\pi(\mu+p)\tau^{-1}\Psi^{-1}A^{[\gamma}B^{\nu]}\ S_{\gamma}\lambda_{\nu}\ . \quad (2.56)$$

When A^{γ} and B^{ν} are constants this becomes

$$D^{m}[\tau^{-1}\beta^{2}\ D_{m}(\alpha/\beta)] = 8\pi(\mu+p)\tau^{-1}\Psi^{-1}\ A^{[\gamma}\ B^{\nu]}\ S_{\gamma}\ \lambda_{\nu}\ , \quad (2.57)$$

where $\alpha \equiv A^{\gamma}\ \lambda_{\gamma}$ and $\beta \equiv B^{\gamma}\ \lambda_{\gamma}$. The choice of $A^{\gamma} = N^{\gamma}$ and $B^{\gamma} = S^{\gamma}$ yields

$$D^{m}[\tau^{-1}\ \Psi^{2}\ D_{m}(\eta/\Psi)] = 0 \quad . \quad (2.58)$$

This equation is a well behaved elliptical differential equation for η/Ψ in any open region not containing points at which either Ψ or τ vanish. According to a theorem due to Hopf[27] η/Ψ will either be a constant or have no extrema in such a region. If a region can be found such that on its boundary η/Ψ is bounded above (below) by zero and unbounded below (above) then η/Ψ will be negative (positive) in the entire region. If, in addition, Ψ has a particular sign in this region then the sign of η will be established.

Hansen and Winicour begin by proving the velocity of light curve, defined as the locus of points where Ψ vanishes, has a single connected component which divides S into two regions where $\Psi < 0$ and $\Psi > 0$. By taking the derivative of eq. (2.16) normal to the axis twice and evaluating the results on the axis one finds that the axis

regularity conditions imply

$$b\,\lambda_{00} = -a^2 \qquad . \quad (2.59)$$

Since a and b are positive this implies that λ_{00} must be negative on the axis. Since λ_{00} and Ψ are equal on the axis it follows that the velocity of light curve cannot intersect the axis.

Because of the causal requirements the velocity of light curve also cannot intersect the fluid. Suppose there exists a region D in S that is bounded by a closed curve on which Ψ vanishes. Because this region D cannot intersect the fluid, eq. (2.57) with the choice $A^{\gamma} = S^{\gamma}$ and $B^{\nu} = (0,0,1)$ becomes

$$D^m[\tau^{-1}\,\lambda_{11}^{2}\,D_m(\Psi/\lambda_{11})] = 0 \qquad . \quad (2.60)$$

The Hopf theorem applied to this equation would require that Ψ/λ_{11} vanish identically in D. This behavior leads Hansen and Winicour to conclude that the curve $\Psi = 0$ cannot bound a region of S and that the velocity of light curve must extend to infinity. By asymptotic flatness, one finds that

$$\Psi \to -1 + (1/2)\Omega^2\rho^2 \qquad , \quad (2.61)$$

far from the fluid. Since $\rho \geq 0$ there can only be a single velocity of light curve asymptotically. Because of this and the fact that no region can be bounded by the curve $\Psi = 0$ the velocity of light curve must have a single connected component which divides S into two regions, $\Psi > 0$ and $\Psi < 0$.

The Hopf theorem can now be applied to eq.(2.58) in a region bounded by the axis and the velocity of light curve. Since the velocity of light curve cannot intersect

the axis and η vanishes there, η/Ψ must also vanish on the axis. Since $\Psi = 0$ on the velocity of light curve, the identity

$$\eta^2 = (1/2)\tau^2 + \lambda_{11}\,\Psi \qquad (2.62)$$

implies that η must have a single sign on the velocity of light curve. By asymptotic flatness η must be positive far from the fluid and, thus, must be positive everywhere on the velocity of light curve. This implies that $\eta/\Psi \to -\infty$ as the velocity of light curve is approached from the interior. Since the Hopf theorem states that η/Ψ cannot have extrema in this region, η/Ψ must be negative which demands that

$$\eta \geq 0 \qquad (2.63)$$

inside the velocity of light curve with the equality holding only on the axis. This argument can be extended to the region outside of the velocity of light curve where $\Psi > 0$. On the boundary of this region which is bounded by the velocity of light curve and some curve far from the fluid, one finds that η/Ψ is positive and by the Hopf theorem must be positive everywhere in this region.

Hansen and Winicour have generated other inequalities involving Killing scalars. The quantity ν, defined by by vector $R^\alpha = (1,\Omega,0)$ as

$$\nu \equiv R^\alpha \lambda_\alpha = \lambda_{00} + \Omega\,\lambda_{01} \quad , \qquad (2.64)$$

is everywhere negative. Within the velocity of light curve this claim follows immediately from the η inequality and causality requirements as seen by writing ν as

$$\nu = \Psi - \Omega\,\eta \quad . \qquad (2.65)$$

For the region outside of the velocity of light curve the Hopf theorem can be applied to the following equation,

$$D^m[\tau^{-1}\ \Psi^2\ D_m(\nu/\Psi)] = 0 \qquad , (2.66)$$

which is obtained from eq. (2.57) by the choice of $A^\alpha = R^\alpha$ and $B^\alpha = S^\alpha$. By eq. (2.65) ν is negative on the velocity of light curve and asymptotically

$$\nu \to -1 - 2\phi \qquad , (2.67)$$

where ϕ is the Newtonian gravitational potential which is much less than unity. Application of the Hopf theorem in the region outside the velocity curve of light demands that ν be negative in this region.

2.5. Integral Inequalities of Rigidly Rotating Perfect Fluids

In this section two classes of inequalities involving integrals performed over the projection of the matching surface onto S will be derived. The usefulness of these inequalities is that they can be applied to the matching problem yielding inequalities involving the interior and exterior parameters which restrict the possible solutions even when there is no detailed knowledge of the interior.

One class of integral inequalities arises from eq. (2.57). By multiplying this equation by an as of yet arbitrary function of α/β and integrating over a region V bounded by the curve $\tau = \varepsilon$, ε being a small positive

constant, and the projection of the matching surface $\mathcal{B}$ as shown in figure one, one finds that

$$\int_V f(\alpha/\beta)\ D^m[\tau^{-1}\ \beta^2\ D_m(\alpha/\beta)]\ dV$$
$$= 8\pi \int_V (\mu+p)\ f(\alpha/\beta)\ \tau\ \Psi^{-1}\ A^{[\mu}\ B^{\nu]}\ S_\mu\ \lambda_\nu\ dV \quad . \quad (2.68)$$

Application of the Gauss theorem to the integral on the left yields

$$\int_C f(\alpha/\beta)\ \tau^{-1}\beta^2 D^m(\alpha/\beta)\ dl_m = \int_V f'(\alpha/\beta)\ \tau^{-1}\beta^2 D^m(\alpha/\beta) D_m(\alpha/\beta) dV$$
$$+ 8\pi \int_V f(\alpha/\beta)\ (\mu+p)\tau^{-1}\Psi^{-1}A^{[\mu}\ B^{\nu]}\ S_\mu\ \lambda_\nu\ dV\ , \quad (2.69)$$

where C is the boundary of V described above, dl_m is the dual of the displacement dx^m along C and f' is the ordinary derivative of f with respect to its argument α/β.

The purpose of the above calculation is as follows. In examining the right side of eq. (2.69) it is seen that the sign of f' determines the sign of the first integral on the right. This is because the norm of D_a is positive definite and τ is intrinsically positive. An inequality will result if A^μ and B^ν are judiciously chosen such that the second integral on the right is positive (negative) while choosing f to be a monotonically increasing (decreasing) function of α/β so that the first integral on the right is also positive (negative). If this can be done then the sign of the integral performed over the boundary of V will be fixed.

For this inequality to be useful when there is no detailed knowledge of the interior, the contribution to the integral from the curve $\tau = \varepsilon$ must vanish in the limit as ε

approaches zero (that is, when this curve approaches the axis). If the axis contribution can be made to vanish for particular choices of A^{μ} ,B^{ν} and f then the integral on the left will reduce to an integral over the projection of the matching surface onto S,$\mathcal{B}$. The resulting integral can then be performed with only knowledge of the exterior.

One class of integral inequalities arises from the choice of $A^{\mu} = N^{\mu}$ and $B^{\nu} = S^{\nu}$. For this choice eq. (2.69) becomes

$$\int_C f(\eta/\Psi)\ \tau^{-1}\ \Psi^2\ D^m(\eta/\Psi)dl_m =$$

$$\int_V f'(\eta/\Psi)\ \tau^{-1}\ \Psi^2\ D^m(\eta/\Psi)D_m(\eta/\Psi)\ \ dV \quad . \quad (2.70)$$

In this case the axis contribution can be made to vanish because of the behavior of η and Ψ near the axis. The axis regularity conditions imply that as the curve $\tau = \varepsilon$ approaches the axis Ψ approaches some finite value while η approaches zero as τ^2. Since $D_a\tau$ is parallel to dl_a on the curve $\tau = \varepsilon$ the axis contribution will vanish provided f vanishes on the axis. The following choice of f,

$$f(\eta/\Psi) = (-\eta/\Psi)^q \quad (2.71)$$

such that $q > 0$, satisfies this condition since the axis regularity conditions demand that η vanish on the axis. This choice then yields the inequality

$$\int_{\mathcal{B}} (-\eta/\Psi)^q\ \tau^{-1}\ \Psi^2\ D^m(\eta/\Psi)\ dl_m < 0 \quad . \quad (2.72)$$

This class of inequalities can be extended to include the

limiting case where q vanishes. This can be seen by writing eq. (2.70) with q = 0 as

$$\int_{\mathcal{B}} \tau \Psi^2 D^m (\eta/\Psi) \, dl_m = \int_{\tau=\varepsilon} \tau^{-1} \Psi^2 \frac{\partial(\eta/\Psi)}{\partial \tau} D^m \tau \, dl_m \quad , \quad (2.73)$$

and noting that the axis regularity conditions imply that the partial derivative of η/Ψ is negative. Thus, the restriction that q be strictly positive can be relaxed to the condition that q be non-negative. One member of this class, the choice of q = 1, has been derived previously by Abramowicz, Lasota and Muchotrzeb[26].

Although one might expect many classes of integral inequalities to be derived for various choices of A^μ, B^ν and f, only one other class of integral inequalities has been derived from eq. (2.69). Following the same arguments as above one finds that the choice of $A^\mu = N^\mu$ and $B^\nu = R^\nu$ and $f(\alpha/\beta) = (-\alpha/\beta)^q$, where $q \geq 0$, yields

$$\int_{\mathcal{B}} (-\eta/\nu)^q \tau^{-1} \nu^2 D^m (\eta/\nu) \, dl_m < 0 \quad . \quad (2.74)$$

This class is very closely related to the above class and is strictly equivalent in the limit as q approaches zero. This can be seen by writing Ψ as $\nu + \Omega \eta$ in eq. (2.72) and expressing the gradient of η/Ψ in terms of the gradient of η/ν. In applying these integral inequalities to Kerr exteriors, the η/Ψ inequalities will impose the strongest restrictions as will be seen in the next chapter.

Although the analysis of the integral inequalities may not be complete, there seems to be no systematic way of

choosing A^{μ} , B^{ν} and f to yield the strongest inequality. No further inequalities arising from eq. (2.69) have been found. To illustrate the difficulties in constructing more integral inequalities, consider the choice $A^{\mu} = (0,1,0)$ and $B^{\nu} = S^{\nu}$. For this choice eq. (2.69) becomes

$$\int_C f(\lambda_{01}/\Psi)\ \tau^{-1}\ \Psi^2\ D^m(\lambda_{01}/\Psi)\ dl_m =$$

$$\int_V f'(\lambda_{01}/\Psi)\ \tau^{-1}\ \Psi^2\ D^m(\lambda_{01}/\Psi)\ D_m(\lambda_{01}/\Psi)\ dV$$

$$-8\pi \int_V f(\lambda_{01}/\Psi)\ (\mu + p)\ \tau^{-1}\ \Omega\ dV \qquad . \quad (2.75)$$

The axis contribution can be made to vanish by choosing f to vanish when its argument vanishes. To establish an inequality f and f' are required to have opposite signs. This is because $\lambda_{01} \leq 0$ which can be proven by means of the Hopf theorem arguments[24]. This cannot happen since f(0) = 0. One could establish the inequality

$$\int_C f(\lambda_{01}/\Psi)\ \tau^{-1}\ \Psi^2\ D^m(\lambda_{01}/\Psi)\ dl_m < 0 \qquad (2.76)$$

by choosing f to be positive and f' to be negative. A simple function satisfying this condition is

$$f(\lambda_{01}/\Psi) = c - (\lambda_{01}/\Psi) \qquad , \quad (2.77)$$

where c is a constant chosen such that

$$c \geq \max(\lambda_{01}/\Psi) \qquad , \quad (2.78)$$

where $\max(\lambda_{01}/\Psi)$ is the maximum value of λ_{01}/Ψ in the interior. The axis regularity conditions imply that the axis contribution is positive and, therefore,

$$\int_{\mathcal{B}} f(\lambda_{01}/\Psi)\, \tau^{-1}\, \Psi^{2}\, D^{m}(\lambda_{01}/\Psi)\, dl_{m} < 0 \qquad , \quad (2.79)$$

for the above choice of f. To explore this inequality detailed information about the interior, namely c, must be known. If the maximum of λ_{01}/Ψ occurs on B then c could be calculated from knowledge of the exterior only. However, the Hopf theorem applied to eq. (2.57) with the choice of $A^{\mu} = (0,1,0)$ and $B^{\nu} = S^{\nu}$ precludes minima from occurring in the interior but does allow the possibility that maxima could exist. Thus, not even the Hopf theorem can save this inequality.

One additional class of integral inequalities can be generated from the field equations. Contracting λ_{α} into eq. (2.33) yields

$$D^{m} D_{m} \tau = 16\pi p\tau \qquad . \quad (2.80)$$

Following an analogous procedure to that described above one finds that

$$\int_{\mathcal{B}} f(\tau)\, D^{m}\tau\, dl_{m} > 0 \qquad (2.81)$$

if f is a positive, monotonically increasing function of τ such that in the limit as τ approaches zero it vanishes.

In the Newtonian limit, both the inequalities, eqs. (2.72) and (2.81), are automatically satisfied. Utilizing the Newtonian limit of τ,

$$\tau \to \sqrt{2}\ \rho \qquad , \quad (2.82)$$

where ρ is the distance from the axis, one finds that eq.

(2.80) becomes

$$\int_{\mathcal{B}} f(\rho)\, \hat{e}_\rho \cdot d\vec{n} > 0 \qquad , (2.83)$$

where $\hat{e}_\rho$ is a unit vector directed away from the axis and $d\vec{n}$ is the outward directed normal to the infinitesimal displacement $d\vec{x}$ along $\mathcal{B}$. For spheroidal configurations the inner product of $\hat{e}_\rho$ and $d\vec{n}$ will be positive and the inequality will be satisfied. Using this Newtonian limit as a guide, the physical content of eq. (2.81) is that the distance from the axis, as measured by τ, must increase, on the average, as one moves from the pole to the equator.

The Newtonian limit of eq. (2.72) can be found by noting that in this limit

$$\Psi \to -1 - 2\phi + \rho^2 \Omega^2 \qquad ,(2.84a)$$

$$\eta \to \Omega \rho^2 \qquad ,(2.84b)$$

$$D^m \eta \to -2\Omega^{-1} \vec{a}_c \qquad ,(2.84c)$$

and,

$$D^m \Psi \to 2(\vec{g} - \vec{a}_c) \qquad ,(2.84d)$$

where $\vec{a}_c$ is the centripetal acceleration and $\vec{g}$ is the Newtonian gravitational field. With these identifications the Newtonian limit of eq. (2.72) becomes

$$\int_{\mathcal{B}} \rho^{-1} f(-\eta/\Psi)\, [\Omega^2 \rho^2 \vec{g} - (1+2\phi)\vec{a}_c] \cdot d\vec{n} > 0 \qquad , (2.85)$$

where $d\vec{n}$ is the normal to the displacement $d\vec{x}$ along $\mathcal{B}$. Since both $\vec{a}_c$ and $\vec{g}$ are directed inward it is the $\vec{g}$ term

which may cause a violation of the inequality. The relation between the two terms can be further explored by examining the pressure condition, eq. (2.45), which in the Newtonian limit becomes

$$\vec{g}\cdot\vec{n} - \vec{a}_c\cdot\vec{n} < 0 \qquad . \quad (2.86)$$

Thus, if $\vec{g}$ is replaced by $\vec{a}_c$ one expects the worst case. With this replacement eq. (2.85) becomes

$$\int_{\mathcal{B}} \rho^{-1} f(-\eta/\Psi)\,[1 + 2\phi - \Omega^2\rho^2]\,\vec{a}_c\cdot d\vec{n} < 0 \qquad . \quad (2.87)$$

The integral inequality is satisfied in the Newtonian limit since $\vec{a}_c\cdot\vec{n} < 0$, $\Omega\,\rho << 1$ and $\phi << 1$. The physical content of this limit is that averaged over the surface the difference between twice the gravitational potential energy and the rotational energy must be less than the rest energy. Since the inequality is automatically satisfied in this limit it is difficult to arrive at a physical interpretation of the inequality without exploring the fully relativistic version. This will be done in the next chapter for a Kerr exterior.

3.0. APPLICATIONS TO KERR INTERIORS

In this chapter the restrictions derived in chapter two will be applied to interiors matched to the Kerr solution as the exterior. The choice of the Kerr exterior is somewhat arbitrary as the results of the preceding chapter hold for any stationary, axisymmetric exterior which is asymptotically flat. The use of the Kerr solution to model the gravitational field of an astrophysical object can be questioned. Hernandez[28] has shown that in the Newtonian limit the Kerr solution has the very special multipole structure

$$q_{2n} = (-1)^{n+1} m^{1-2n} J^{2n} \quad , \quad (3.1)$$

where q_{2n} is the $2n^{\underline{th}}$ coefficient of the Legendre series for the Newtonian potential, m is the mass and J is the angular momentum. Because of this very special relationship between the multipole moments and the angular momentum, it is unlikely that the Kerr solution describes any realistic astrophysical system[29,30]. The larger Tomimatsu-Sato family of solutions[31], which are stationary, axisymmetric and asymptotically flat, have a more general multipole structure. However, the Kerr solution, which is a member of this family, gives the simplest physical insight into the restrictions derived in the preceding chapter. Additional motivation for using a Kerr exterior is provided by the investigations reviewed in chapter one which indicate that

the Kerr exterior may be obtained in the extreme relativistic limit.

3.1. The Kerr Solution

This two parameter solution of the vacuum field equations, discovered in 1963 by Kerr[32], is characterized by the parameters m and a. In Boyer-Lindquist coordinates the Kerr metric takes the form

$$ds^2 = \rho^2(\Delta^{-1}dr^2 + d\theta^2) + (r^2 + a^2)\sin^2\theta\, d\phi^2 - dt^2 + 2mr\rho^{-1}(a\sin^2\theta\, d\phi - dt)^2 \quad , \quad (3.2a)$$

where

$$\rho^2 = r^2 + a^2\cos^2\theta \quad , \quad (3.2b)$$

and

$$\Delta = r^2 - 2mr + a^2 \quad . \quad (3.2c)$$

As seen from this form the Kerr solution reduces to the Schwarzschild solution when a vanishes. By comparison with the linear theory one finds that m represents the total mass of the system and a represents the angular momentum of the system per unit mass.

From eqs. (3.2) it is seen that this form of the metric becomes singular when either Δ or ρ vanishes. ρ vanishes only in the equatorial plane (i.e.,when $\theta = \pi/2$) when $r = 0$. This is a true singularity in the spacetime as the curvature scalar diverges when ρ is zero.

At first glance one might believe that this is a point singularity. However, it is actually a ring. This

can be seen by transforming to Cartesian-like spatial coordinates (x,y,z) defined by

$$x + iy = (r + ia)\exp(i\phi) \quad , \quad (3.3a)$$

and

$$z = r\cos\theta \quad . \quad (3.3b)$$

In these coordinates the metric takes on the Kerr-Schild form[33]

$$ds^2 = dx^2 + dy^2 + dz^2 - dt^2$$

$$+ \frac{2mr^3}{r^4+a^2z^2}\left\{\frac{r(xdx-ydy) - a(xdy-ydx)}{r^2+a^2} + \frac{zdz}{r} + dt\right\}^2 \quad . (3.4)$$

From eqs. (3.3) one finds that r is determined by solving the quartic

$$r^4 - (x^2 + y^2 + z^2 - a^2)r^2 - a^2z^2 = 0 \quad . \quad (3.5)$$

Inspection of this equation shows that in the equatorial plane the vanishing of r corresponds to a disk where $x^2+y^2 \leq a^2$. In these coordinates the curvature scalar diverges only on the boundary of the disk where $x^2+y^2=a^2$.

The Kerr solution can be extended to negative values of r. By identifying the top of the r=0 disk in the region of the spacetime where r is positive with the bottom of the r = 0 disk in the region of the spacetime where r is negative and doing likewise with the top of the disk in the negative r region with the bottom of the disk in the positive r region one finds two distinct regions connected by a "wormhole" formed by the disk. This "wormhole" does introduce problems with causal requirements. One finds that the rotational Killing vector field becomes timelike for

negative values of r near the singularity giving rise to acausal closed timelike curves in the spacetime. Carter[34] has shown that for the case a > m these closed timelike curves can be deformed to pass through any point in the extended spacetime.

The vanishing of Δ does not result in a true singularity of the spacetime but a coordinate singularity associated with the Boyer-Lindquist coordinates. When the radial coordinate takes the value

$$r_{\pm} = m \pm \sqrt{m^2 - a^2} \quad , \quad (3.6)$$

Δ vanishes. These two surfaces are null two surfaces and are the event horizons of the Kerr solution. Note that for the case a > m there are no real solutions of $\Delta = 0$; and, thus, there are no event horizons. This behavior leads to a naked singularity for this case.

For the case a < m there is yet more structure. On the surface defined by

$$r(\theta) = m + \sqrt{m^2 - a^2\cos^2\theta} \quad , \quad (3.7)$$

the timelike Killing vector becomes null. This surface is timelike everywhere except at the poles where it coincides with the outer horizon. The physical interpretation of this surface is that no observer inside this surface can remain stationary as viewed by an observer in an asymptotic Lorentz frame. The reason for this is that the velocity of a static observer is proportional to the timelike Killing vector. This surface is known as the static limit and the region between the static limit and the outer horizon is

known as the ergosphere due to the fact that negative energy states exist in this region. These negative energy states allow processes which can drain the rotational energy from the Kerr black hole[35].

3.2. The Matching Surface

In this section the matching surface will be investigated. As in Newtonian theory the matching surface will be defined to be the surface where the pressure vanishes. By the relativistic version of Von Zeipel's theorem the matching surface is also a surface of constant redshift. This allows the matching surface to take on an explicit form.

In Boyer-Lindquist coordinates the Killing vector fields are $\xi^m_0 = (1,0,0,0)$ and $\xi^m_1 = (0,0,0,1)$ which implies that

$$\lambda_{00} = g_{00} = -1 + 2mr/\rho^2 \quad , \quad (3.8a)$$

$$\lambda_{01} = g_{03} = -2mra\sin^2\theta/\rho^2 \quad , \quad (3.8b)$$

and

$$\lambda_{11} = g_{33} = (r^2 + a^2)\sin^2\theta + 2mra^2\sin^4\theta/\rho^2 \quad , \quad (3.8c)$$

where ρ is defined as above. With these explicit forms Boyer[25] demonstrated that the generalization of Von Zeipel's theorem becomes

$$-1 + \Omega^2(r^2 + a^2)\sin^2\theta + 2mr(1-a\Omega\sin^2\theta)^2/\rho^2 = \Psi_o \quad , \quad (3.9)$$

where Ψ_o is the redshift factor of the matching surface.

Solutions of this equation for a given Kerr exterior parameterized by m and a and a particular interior parameterized by Ψ_o and Ω give the allowable boundaries of the fluid. In the calculations it is convenient to replace Ψ_o by K defined as

$$K \equiv 1 + \Psi_o \quad . \quad (3.10)$$

Note that in order for the fluid elements on the surface to follow a timelike trajectory

$$K \leq 1 \quad . \quad (3.11)$$

It is also convenient to view the equation for the matching surface as a quartic equation in r parameterized by m, a, K and Ω,

$$P(r,\theta;m,a,K,\Omega) = 0 \quad , \quad (3.12)$$

where

$$P = r^4\Omega^2\sin^2\theta + r^2[a^2\Omega^2\sin^2\theta(1+\cos^2\theta) - K]$$

$$+ 2mr(1-a\Omega\sin^2\theta)^2 + a^2\cos^2\theta\,(a^2\Omega^2\sin^2\theta - K) \quad . \quad (3.13)$$

Although no closed-form solution in the form $r = r(\Theta)$ is known, useful information can be obtained by investigating special cases of eq. (3.12). On the axis the surface equation reduces to a quadratic in r with solutions

$$R_\pm = (m/K) \pm \sqrt{(m/K)^2 - a^2} \quad . \quad (3.14)$$

The quartic also has a positive root $r \to \infty$ associated with the degeneracy $\sin\theta \to 0$. The condition that the pressure increase inward, eq. (2.45), is only satisfied for R_+. A necessary condition that the boundary have spherical topology is that solutions exist at the poles which demands

$$K \leq m/a \quad . \quad (3.15)$$

This will be refered to as the Boyer polar condition.

At the equator eq. (3.12) reduces to the cubic equation

$$r^3\Omega^2 + r^2(a^2\Omega^2 - K) + 2m(1-a\Omega)^2 = 0 \quad , \quad (3.16)$$

and a root at r = 0. The positive solutions of this cubic are

$$R_k = 2\left[\frac{1}{3}\left(\frac{K}{a^2\Omega^2} - 1\right)\right]^{1/2} \cos[(\alpha+2\pi k)/3] \quad , \quad (3.17)$$

where k = 0 or 2 and

$$\cos\alpha = -m\Omega(1-a\Omega)^2[3/(K-a^2\Omega^2)]^{3/2} \quad , \quad (3.18)$$

such that α is chosen to be in the third quadrant. For R_k to be real cos α must be less than or equal to one, which implies that

$$K \geq a^2\Omega^2 + 3(m\Omega)^{2/3}(1-a\Omega)^{4/3} \quad . \quad (3.19)$$

This inequality will be refered to as the Boyer equatorial condition. The pressure condition is satisfied only for k = 0.

The pressure condition implies that if any boundary with spherical topology exists it must pass through R_+ at the pole and R_0 at the equator. Thus, eqs. (3.15) and (3.19) represent necessary conditions for the existence of a spheriodal boundary. The question of whether these conditions represent sufficient conditions for the existence of a continuous spheroidal boundary at intermediate values of θ has not been resolved. The work of deFelice', Nobili and Calvani[36] and my own extensive numerical studies seem to imply that Boyer conditions do represent sufficient

conditions. Attempts were made to solve the quartic by means of the quartic algorithm[37]. However, the application to the quartic became so complicated that it was abandoned.

The numerical examples which numbered in the tens of thousands showed the following behavior when the Boyer conditions were satisfied. The positive solutions of eq. (3.12) define three non-intersecting surfaces: one which connects R_- at the pole to r = 0 at the equator, one which connects R_+ at the pole to R_0 at the equator, and one which tends to infinity at the pole connecting to R_2 at the equator. An attempt was made to prove the existence of these surfaces by applying Sturm's theorem[38] which would show that eq.(3.12) has three non-degenerate, positive roots at all intermediate polar angles. As in the case of the attempt to solve the quartic, the analysis became extremely complex and was finally abandoned after the results were established for some limited ranges of the parameters. While the possibility that additional inequalities could arise from further attempts, the numerical studies imply that the Boyer conditions are sufficient conditions for the existence of boundaries with spherical topology.

As demonstrated by deFelice', Nobili and Calvani[36] the condition that the pressure increase as one moves inward into the fluid from the matching surface is also consistent with spheroidal configurations which have an internal cavity defined by the surface connecting R_- at the pole to r = 0 at the equator. In addition, if the Boyer polar condition is

violated when a > m then toroidal configurations appear defined by a surface connecting r = 0 on the equator to R_0 on the equator. As a is increased from a value less than m to a value greater than m the spheroidal configurations with cavity transform smoothly into the toroidal configurations. Any physical interpretation of these two classes of configurations lacks credibility as the ring singularity at r = 0 appears on the inner surface. Because of this fact and the multiple connectedness associated with the disk at this point only spheroidal configurations without the internal cavity will be considered here.

3.3. Application of the Algebraic Inequalities

The algebraic inequalities derived in Chapter Two will now be applied to the matching surface. The virial theorem offers no restrictions that are not already contained in the combination of the timelike flow condition, eq. (3.11), and the Boyer equatorial condition. The maximum angular velocity allowed by these two conditions is a solution of the sixth order equation

$$(1-a^2\Omega^2)^3 = 27(m\Omega)^2(1-a\Omega)^4 \quad . \quad (3.20)$$

Application of Sturm's theorem on the interval allowed by the virial theorem (0,1/2a) shows that there is always one root in this interval when a < m. Thus, the Boyer equatorial condition is stronger than the virial theorem. The same is true for a > m when the timelike flow condition

is replaced by the Boyer polar condition. In the case where $a = m$ both the Boyer equatorial condition and the virial theorem imply that $a\Omega < 1/2$.

As was stated in section 2.4. the ν inequality is satisfied within the velocity of light curve whenever the η inequality is satisfied. Thus, it is sufficient to invesitgate the restrictions arising from the η inequality. Due to the lack of a closed-form solution for the matching surface it seems that the η inequality can not be applied to an arbitrary point on the surface. However, a closed-form inequality among the parameters which is a necessary and sufficient condition for the η inequality to be satisfied everywhere on the matching surface does exist.

A necessary condition can be found by examining the behavior of η near the pole. The axis regularity conditions imply that both η and the first in-surface derivative must vanish on the axis and, therefore, also at the pole. If η is to be positive near the axis then the second in-surface derivative must be non-negative. The necessary condition found in this manner will also be a sufficient condition for η to be non-negative everywhere on the matching surface if η increases monotonically as one moves from the pole to the equator. The fact that η does increase monotonically is seen by calculating the partial derivative of η with respect to $\sin^2\theta$ and evaluating the result on the matching surface by means of eqs. (3.12) and (3.13). After some manipulation the calculation yields

$$\frac{\partial \eta}{\partial(\sin^2\theta)} - \frac{\eta \sin^{-4}\theta}{(1-a\Omega\sin^2\theta)}$$

$$-\{(1-K)(K-a^2\Omega^2\sin^4\theta)+[(K-1)a\Omega\sin^2\theta+\eta\sin^{-2}\theta(1-a^2\Omega^2\sin^4\theta)]^2\}$$

$$\times \frac{2a\Omega r}{P'(1-a^2\Omega^2\sin^4\theta)} \quad , (3.21)$$

where P' is the partial derivative of P with respect to r. Inspection of the right side of this equation shows that it is positive due to the timelike condition on K, the virial theorem, the Boyer equatorial condition and the fact that the pressure condition eq. (2.45) requires P' to be negative. Thus, η is a monotonically increasing function as one moves from the pole to the equator. The condition that the second in-surface derivative be non-negative is equivalent to

$$\frac{\partial \eta}{\partial(\sin^2\theta)} \geqslant 0 \quad , (3.22)$$

at the pole. By calculating this quantity and substituting the polar radius written in terms of the parameters into the result one finds

$$\frac{2m\Omega}{aK^2}\left\{\frac{m}{K} + \left(\frac{m^2}{K^2} - a^2\right)^{1/2}\right\} \geqslant 1 \quad , (3.23)$$

as a necessary and sufficient condition for η to be non-negative everywhere on the matching surface. It should be noted that this condition is not sufficient to guarantee that $\eta \geq 0$ globally. The local nature of this result is also indicated by the fact that the condition that the pressure be positive is required only in the neighborhood of the matching surface. In fact, this inequality may be

satisfied for configuartions containing interior regions in which not only is the pressure negative but the positive energy condition, eq. (2.10), may be violated.

3.4. Application of the Integral Inequalities

The analysis of the integral inequalities in eqs. (2.72), (2.74) and (2.81) is a problem that poses more difficulty than the analysis of the algebraic inequalities for three reasons: the seemingly ever present lack of a closed form expression for the matching surface, the fact that the integral inequalities are actually classes of inequalities with one member for each choice of f, and the lack of a meaningful Newtonian limit to use as a guide. The first two problems can be overcome by resorting to purely numerical techniques to solve eq. (3.12) for the matching surface and performing the integrals. The problem of determining the strongest restrictions due to the integral inequalities then becomes a straightforward but time consuming parameter study.

The results of this parameter study are as follows. The strongest class of restrictions comes from the η/Ψ integral inequalities eq. (2.72) while the η/ν inequalities eq. (2.74) are only slightly weaker except in the limit of $q = 0$ where the two inequalities agree as noted in section 2.4. The class of integral inequalities eq. (2.81) based on the τ equation made no restrictions to numerical accuracy. The strongest restriction of the η/Ψ class of inequalities

came from the choice of q = 0 as shown in figure two. Although not shown in this figure for the sake of clarity, many choices of q were used yielding the result that as q is smoothly increased the range of allowed parameters also smoothly increases.

The fact that the choice q = 0 yields the strongest restrictions is a quite fortunate result as the field equations will allow this integral to be performed analytically. To see this, note that this inequality is based upon the following combination of the field equations:

$$D_m^m [\tau^{-1} \Psi^2 D_m (\eta/\Psi)] = 0 \quad . \quad (3.24)$$

If this equation is integrated over A, any closed region of S, and the Gauss theorem is utilized one finds that

$$\int_{\partial A} \tau^{-1} \Psi^2 D_m^m (\eta/\Psi) \, dl_m = 0 \quad , \quad (3.25)$$

where ∂A is the boundary of A. If this region A is chosen to be the region bounded by $\mathcal{B}$, the projection of the matching surface on S, portions of the axis and a curve at constant r far from the fluid as shown in figure three then

$$\int_{\mathcal{B}} \tau^{-1} \Psi^2 D_m^m (\eta/\Psi) \, dl_m = \int_{\mathcal{A}} \tau^{-1} \Psi^2 D_m^m (\eta/\Psi) \, dl_m + \int_R \tau^{-1} \Psi^2 D_m^m (\eta/\Psi) \, dl_m \quad , \quad (3.26)$$

where $\mathcal{A}$ denotes the integration along the axis from the pole R_+ to some large value of r = R, and R denotes the integration along the curve r = R from the north pole to the

south pole. With this choice of A both the integrals on the right of eq. (3.26) can be performed analytically with the results

$$\int_A \tau^{-1} \Psi^2 D_m^m (\eta/\Psi)\, dl$$

$$= 2^{3/2}\{\Omega(R-R_+) + ma[(R^2+a^2)^{-1} - (R^2+a^2)^{-1}]\} \quad , \quad (3.27)$$

and

$$\int_R \tau^{-1} \Psi^2 D_m^m (\eta/\Psi)\, dl$$

$$= -2^{3/2}\Omega[R - m(3-2a\Omega)] + \mathcal{O}\left(R^{-1}\right) \quad . \quad (3.28)$$

Since the divergenceless character of $\tau^{-1} \Psi^2 D_m^m (\eta/\Psi)$ allows the boundary of A to be freely deformed with no change in the value of the integral in eq. (3.25) R can approach infinity yielding

$$\int_B \tau^{-1} \Psi^2 D_m^m (\eta/\Psi) dl = 2^{3/2}[m\Omega(3-2a\Omega) - \Omega R_+ - ma(R_+^2+a^2)^{-1}] \quad . \quad (3.29)$$

Thus, the integral inequality eq. (2.72) becomes

$$4maR_+\Omega^2 + 2R_+(R_+-3m)\Omega + aK \geq 0 \quad . \quad (3.30)$$

This is the strongest known restriction arising from any known integral inequality. Like the η inequality, eq. (3.23), this restriction does not require the positive energy condition eq. (2.10) to hold. Thus, eq. (3.30) may be satisfied for configurations containing interior regions in which either the pressure is negative or eq. (2.10) is violated.

This technique of deforming $\mathcal{B}$ to a curve consisting of portions of the axis and a semicircle of infinite radius can also be applied to the τ integral due to the fact that in the exterior τ is harmonic. When f is chosen to be a constant the τ inequality becomes

$$R_+ \geq m \qquad . \quad (3.31)$$

Simple manipulations with eqs. (3.14) and (3.15) show that this inequality is weaker than the Boyer polar condition. Thus, the τ inequalities are automatically satisfied for spheroidal configurations.

3.5. Overall Restrictions on Kerr Interiors

The strongest restrictions on rigidly rotating, perfect fluid Kerr interiors come from a combination of the Boyer conditions eqs. (3.15) and (3.19), the η inequality of Hansen and Winicour eq. (3.23), and the η/Ψ integral inequality eq. (3.30). Three distinct behaviors which depend on the value of the ratio a/m are evident. When $a < m$ the interior parameters are restricted to a triangular region in the (Ω,K) plane as seen in figures 4 through 12. In these figures the boundaries of the region of allowed parameters are the η inequality which connects the origin to the top vertex of the triangle at $K = 1$, the integral inequality which connects the top vertex to the vertex at the right, and the Boyer equatorial condition which connects the right vertex to the origin. As a approaches m the relative importance of the integral

inequality diminishes. In the limiting case where a = m, shown in figure 13, the integral inequality poses no restrictions on the interior parameters. On these graphs configurations above the dotted line have ergotoroids emerging from the fluid. Their existence is consistent with the findings of Butterworth and Ipser[11,12]. It should be noted that for all cases where a < m ergotoroids do appear; however, the regions for a << m are too small to indicate on the figures.

The prominent feature of these cases is the intersection of the η inequality and the integral inequality at K = 1. As K approaches one the matching surface becomes null and, therefore, represents the extreme relativistic limit. In this limit the η inequality becomes

$$\Omega \geq (a/2m)[m + (m^2-a^2)^{1/2}]^{-1} \quad . \quad (3.32)$$

The right side is the angular velocity of the Kerr horizon[39] Ω_H. Thus, the η inequality becomes

$$\Omega \geq \Omega_H \quad . \quad (3.33)$$

Performing the same limit on the integral inequality yields

$$\Omega \leq \Omega_H \quad . \quad (3.34)$$

For the case where a = m the Boyer equatorial condition also implies eq. (3.34). Thus, combining the η inequality and the integral inequality (or the Boyer for a = m) yields a very simple result: For each Kerr exterior such that a ≤ m, there exists only one possible extreme relativistic

configuration characterized entirely by its angular velocity which is equal to the angular velocity of the Kerr horizon. The conclusion drawn from this result is that the matching surface must approach the Kerr horizon in the extreme relativistic limit.

Another feature of the restrictions for cases where $a \leq m$ is the formation of a step-like behavior of the integral inequality in the limit as $a \to 0$ (i.e.,as the exterior approaches the Schwarzschild solution) which can be seen in figures 4 through 7. Although no restrictions are placed on non-rotating configurations ($\Omega = 0$) due to the existence of the intersection of the η inequality and the integral inequality at $K = 1$, there is a limiting value of K for rotating configurations. As a approaches zero the integral inequality viewed as a quadratic in R_+ becomes

$$R_+ \geq 3m \quad , \quad (3.35)$$

which implies

$$K \leq 2/3 \quad , \quad (3.36)$$

as demonstrated in the figures. The implications of the behavior of the restrictions in this static limit of a spherically symmetric fluid with a Schwarzschild exterior will be discussed in the next chapter.

When $a > m$ the integral inequality poses no restrictions on the interior parameters. The restrictions arise from the η inequality and the Boyer conditions. For cases where $m < a \lesssim 5.23094\ m$ only the η inequality and the Boyer equatorial condition restrict the interior parameters

as seen in figures 14 through 16. In these figures the upper curve is the η inequality and the lower curve is the Boyer equatorial condition. At $a \approx 5.23094$ m the Boyer polar condition begins to play a role in restricting the interior parameters as seen in figure 17. In this figure the dotted line represents the Boyer polar condition. As seen in figures 18 through 21 the allowed parameters are restricted to a triangular region in the (Ω,K) plane with the boundaries defined by the η inequality at the left, the Boyer polar condition at the top and the Boyer equatorial condition at the right. One should note that the scales of the axes on figures 18 through 21 are decreasing as a becomes much greater than m. This shows that only nearly Newtonian ($K << 1$) and slowly rotating ($\Omega << 1$) spheroidal configurations are allowed in this limit.

4.0. Concluding Remarks

4.1. Existence vs. Stability

As demonstrated in the last chapter, the strongest restrictions do not rule out rotating fluid configurations with arbitrarily high redshift. This is a somewhat surprising result when one considers that the stability arguments Buchdahl[8] and Bondi[9] imply that $z \leq 2$ for non-rotating configurations. To understand this apparent dichotomy the behavior of the integral inequality in the static limit of a spherically symmetric fluid with a Schwarzschild exterior will be derived and compared to the slowly rotating models discussed in chapter one. This comparison will show that the restrictions of chapter three are not as strong as those based on stability criteria.

The static limit is equivalent to considering perturbations to a spherically symmetric fluid with a Schwarzschild exterior. In this limit, to first order in a and Ω, the surface is spherical as eq. (3.13) becomes $K = 2m/R$, where R represents the value of the Schwarzschild coordinate r at the matching surface. In terms of R the η inequality, eq. (3.23), reduces to

$$R^3\Omega \geq 2ma \tag{4.1}$$

and the integral inequality, eq. (3.30), reduces to

$$R^2(R-3m)\Omega + ma \geq 0 \quad . \tag{4.2}$$

Although the η inequality implies that slowly rotating ($\Omega<<1$) configurations have little angular momentum ($a<<1$),

it does not exclude rotating configurations with zero angular momentum. Such configurations would not appear possible without negative density or pressure regions. However, as noted in chapter three, positive density and pressure are not globally required for the inequalities to hold.

The physical content of eqs. (4.1) and (4.2) can be found by introducing the moments of inertia of the fluid and the spacetime. The moment of inertia of the fluid can be written as $I = \alpha m R^2$ where α represents the matter distribution which can vary from a mass point ($\alpha=0$) to a thin shell of radius R ($\alpha=1$). The moment of inertia of a nearly static spacetime ($J<<1$) as defined by Hartle[39] is

$$I \equiv \left.\frac{\partial J}{\partial \Omega}\right|_{\Omega=0} \quad . \quad (4.3)$$

This allows J to be written as $J = I\Omega$. By using the Kerr relationship, $J = ma$, and equating the two moments of inertia the Kerr parameter a may be written as

$$a = \alpha \Omega R^2 \quad . \quad (4.4)$$

This allows the inequalities to be written entirely in terms of the unperturbed static background quantities m and R. Substitution of eq. (4.4) into the inequalities shows that the η inequality is automatically satisfied and eq. (4.2) becomes $R \leq (3 - \alpha)m$, which implies that

$$K \leq 2/(3 - \alpha) \quad . \quad (4.5)$$

Thus, in the static limit there exists a finite upper bound to the redshift of rotating models which depends on the matter distribution as represented by α. In the thin shell

limit ($\alpha \to 1$) the redshift becomes unbounded as expected from the models of Brill and Cohen[1] and of De La Cruz and Israel[2].

The slowly rotating incompressible fluid models of Chandrasekhar and Miller[6] provide a much more realistic case with which to explore the restriction. They found that α ranges from the Newtonian value of 2/5 to an upper limit of approximately 4/5. This upper limit to α occurs when the unperturbed fluid sphere has the minimum radius, 9m/4, allowed by the stability requirement that the pressure increase inwardly . This lower limit for R is a special case of the results of Buchdahl[8] and Bondi[9]. For this minimum radius K = 8/9 whereas the integral inequality eq. (4.5) with α = 4/5 yields an upper limit of 10/11. Thus, there are configurations allowed by the integral inequality (in the range $8/9 < K < 10/11$) which contain a region or regions in which the pressure must increase outward . This shows that in the static limit the restrictions based upon stability must be stronger than those based upon existence.

The limit coming directly from the integral inequality K = 2/3 corresponds to the case where α = 0 for which the moment of inertia vanishes. In this case it is clear that some negative density or pressure region must exist to preclude the formation of a horizon. Since the condition that the density and pressure be positive is a sufficient but not a necessary condition for validity of the inequalities such behavior is not excluded. Again, the

conclusion is that restrictions based upon stability must be stronger than those based upon existence.

4.2. Future Trips into the Unknown which Lead Us back to Reality

In this concluding section further explorations will be discussed. Of all of these, the question of stability must stand out. Although it seems that stability requirements must further restrict the allowed interiors, the central issue is to what degree will they pose additional restrictions. The static limit implies that the restrictions due to existence are only slightly weaker than those due to stability. Could it be that the Bondi-Buchdahl $z = 2$ limit imposed on non-rotating fluids is misleading in the rotating case? If so, the redshift controversy[40,41] of extragalactic astronomy could once again be revived. However, there is no known generalization of the $z = 2$ limit for rotating fluids.

Further investigations are also suggested by the assumptions upon which the restrictions are based. One key limitation is the fact that only rigid rotations were considered. Generalizations to differential rotation for some of the algebraic inequalities have been found[24]. However, these results have not yet been proven for finite sources. The major difficulty in extending the Hopf theorem arguments to the case of differential rotation is that there is apparently no natural way of defining Ω outside the fluid. As it appears unlikely that astrophysical objects

rotate rigidly, the question of the effects of differential rotation merit further study.

Another limitation arises from the assumption that only the relatively simple model of uncharged perfect fluids was considered. Bekenstein and Oron[42,43] have made initial investigations into the question of utilizing rigidly rotating but charged fluids as a model for neutron stars. Although no restrictions were imposed by their work, their generalization of Von Zeipel's theorem implies that the surface can unambiguously be defined by an equation similar to the uncharged case but having an additional pressure term, $B^2/8\pi$, due to the magnetic pressure. As their model represents the known physics of neutron stars very well, an attempt to match this type of interior to an appropriate exterior such as the Kerr-Newman solution[44] or the Esposito-Witten family of solutions[45] would be very interesting. However, the generalizations of the global algebraic inequalities and the integral inequalities might be very difficult to generate due to the fact that the magnetic field introduces circulation, as measured by the fields c_A defined in eq. (2.24), to the spacetime. This addition destroys the orthogonal transitivity of the spacetime and the purely elliptical nature of the field equations. This consideration brings us to an important question. How does circulation in a spacetime which can be generated either by a magnetic field or by simple convection effect the restrictions? The added complexity of the field

equations clouds this issue but it merits further consideration.

As with most scientific endeavors this work leads to more questions than it answers. However, it is my hope that this very small step forward may provide motivation for further investigations which will give us a better understanding of the beauty that is ours to see on a clear night.

Acknowledgments

I wish to thank my advisor, Jeffrey Winicour, to whom I am grateful for his incredible patience. I would also like to thank the Theoretic Applications Division of the Los Alamos National Laboratory for their support and hospitality during my stay at the Lab. I truly appreciate the use of some of their facilities which made much of this work easier. A special thanks goes to the superintendents and staffs of Yellowstone National Park and the Gallatin and Santa Fe National Forests who provided a refuge away from city lights for viewing the night sky, which is what this is all about.

References Cited

1. D. R. Brill and J. M. Cohen, Phys. Rev. 143, 1011 (1966).

2. V. De La Cruz and W. Israel, Phys. Rev. 170, 1187 (1968).

3. T. Lewis, Proc. Roy. Soc. 136A, 176 (1932).

4. J. M. Bardeen and R. V. Wagoner, Astrophys. J. 167, 359 (1971).

5. J. M. Bardeen, in Black Holes, edited by C. deWitt and B. S. deWitt (Gordon and Breach, New York, 1973).

6. S. Chandrasekhar and J. C. Miller, Mon. Not. R. Astron. Soc. 167, 63 (1974).

7. J. B. Hartle and K. S. Thorne, Astrophys. J. 153, 807 (1968).

8. H. A. Buchdahl, Phys. Rev. 116, 1027 (1959).

9. H. Bondi, Proc. Roy. Soc. 282A, 303 (1964).

10. S. Bonnazzola and J. Schneider, Astrophys. J. 191, 273 (1974).

11. E. M. Butterworth and J. R. Ipser, Astrophys. J. 200, L103 (1975).

12. E. M. Butterworth and J. R. Ipser, Astrophys. J. 204, 200 (1976).

13. W. Roos, Gen. Rel. Grav. 7, 431 (1976).

14. J. L. Friedman and B. F. Schutz, Astrophys. J. 199, L157 (1975).

15. J. L. Friedman and B. F. Schutz, Astrophys. J. 200, 204 (1975).

16. S. Chandrasekhar, Astrophys. J. 161, 571 (1970).

17. B. Carter, in Black Holes, edited by C. DeWitt and B. S. DeWitt (Gordon and Breach, New York, 1973), p. 151.

18. A. Komar, Phys. Rev. 113, 934 (1959).

19. B. Carter, Commun. Math. Phys. 17, 233 (1970).

20. C. W. Misner, K. S. Thorne and J. A. Wheeler, Gravitation (W. H. Freeman and Co., San Francisco, 1973), p. 567.

21. R. Geroch, J. Math. Phys. 13, 394 (1972).

22. R. O. Hansen and J. Winicour, J. Math. Phys. 16, 804 (1975).

23. W. Kinnersley, in The Seventh International Conference on General Relativity and Gravitation, edited by G. Shaviv and J. Rosen (J. Wiley and Sons, New York, 1975).

24. R. O. Hansen and J. Winicour, J. Math. Phys. 18, 1206 (1977).

25. R. H. Boyer, Proc. Camb. Phil. Soc. 68, 199 (1965).

26. M. A. Abramowicz, J. P. Lasota and B. Muchotrzeb, Commun. Math. Phys. 47, 109 (1976).

27. R. Courant and D. Hilbert, Methods of Mathematical Physics, Vol. 2 (J. Wiley and Sons, New York, 1962), p.326.

28. W. C. Hernandez, Phys. Rev. 159, 1070 (1967).

29. K. S. Thorne, in Gravitation and Cosmology, Proceedings of the International School of Physics Enrico Fermi, Course 47, edited by R. K. Sachs (Academic Press, New York, 1971).

30. K. S. Thorne (private communication).

31. A. Tomimatsu and H. Sato, Prog. Theor. Phys. 50, 95 (1973).

32. R. P. Kerr, Phys. Rev. Lett. 9, 237 (1963).

33. B. Carter, in Black Holes, edited by C. DeWitt and B. S. DeWitt (Gordon and Breach, New York, 1973), p.109.

34. B. Carter, Phys. Rev. 174, 1559 (1968).

35. R. Penrose, Nuovo Cimento 1, 252 (1969).

36. F. de Felice', L. Nobili and M. Calvani, Astron. Astrophys. 47, 309 (1976).

37. I. N. Bronshtein and K. A. Semendyayev, A Guide Book to Mathematics (MacMillan, New York, 1964), p. 163.

38. I. N. Bronshtein and K. A. Semendyayev, op. cit., p.166.

39. J. B. Hartle, Astrophys. J. 167, 359 (1967).

40. G. Burbidge, in L'evolution des Galaxies et ses Implications Cosmologiques, edited by C. Balkowski and B. E. Westerlund (Centre National de la Recherche Scientifique, Paris, 1977), pp.555-561.

41. M. J. Rees, in L'evolution des Galaxies et ses Implications Cosmologiques, edited by C. Balkowski and B. E. Westerlund (Centre National de la Recherche Scientifique, Paris, 1977), pp.563-568.

42. J. D. Bekenstein and E. Oron, Phys. Rev. D 18, 1809 (1978).

43. J. D. Bekenstein and E. Oron, Phys. Rev. D 19, 2827 (1979).

44. E. T. Newman, E. Couch, K. Chinnapared, A. Exton, A. Prakash and R. Torrence, J. Math. Phys. 6, 918 (1965).

45. F. P. Esposito and L. Witten, Phys. Rev. D 8, 3302 (1973).

Figure Captions.

Figure One. The Region of Integration V. It is bounded by by $\mathcal{B}$, the projection of the physical matching surface onto S, and the curve $\tau = \varepsilon$ (dashed line).

Figure Two. The Integral Inequalities in the Limit as $q \to 0$. The curves labeled ra through re represent the integral inequality eq. (2.72) for choice of q ranging from zero to one. The strongest restriction comes from the curve ra which corresponds to the choice $q = 0$.

Figure Three. The Region of Integration A. It is bounded by $\mathcal{B}$, the projection of the physical matching surface onto S, $\mathcal{A}$, portions of the axis extending from the poles to some large value, R, of the radial coordinate and the curve $r = R$.

Figure Four. Restrictions for $a/m = 10^{-5}$. Only values of the parameters within the triangular region of the $(m\Omega,K)$ plane are allowed. In this case the step-like behavior of the integral inequality has become quite evident. The η inequality rises nearly vertically from the origin to intersect the integral inequality at $K = 1$ forming a very thin peak. The Boyer equatorial condition begins at the origin and intersects the integral inequality at $(m\Omega,K) = (0.104757,0.666667)$.

Figure Five. Restrictions for $a/m = 10^{-4}$. Although not apparent, the η inequality rises nearly vertically to meet

the integral inequality at K = 1 near Ω = 0. The Boyer equatorial condition (lower curve) intersects the integral inequality at ($m\Omega$,K) = (0.104765,0.666695).

Figure Six. Restrictions for a/m = 10^{-3}. Although not apparent the η inequality rises nearly vertically to meet the integral inequality at K = 1 near Ω = 0. The Boyer equatorial condition intersects the integral inequality at ($m\Omega$,K) = (0.104845,0.666949).

Figure Seven. Restrictions for a/m = 10^{-2}. The η inequality (on the left) has now become apparent. The integral inequality and the Boyer equatorial condition intersect at ($m\Omega$,K) = (0.105647,0.669498).

Figure Eight. Restrictions for a/m = 0.1. The values of $m\Omega$ and K are restricted to the area bounded on the left by the η inequality and the integral inequality (top right) and the Boyer equatorial condition (bottom right) which intersect at ($m\Omega$,K) = (0.114251,0.695754).

Figure Nine. Restrictions for a/m = 0.3. The values of the parameters are restricted to the area bounded on the left by the η inequality and the integral inequality (upper right) and the Boyer equatorial condition (lower right) which intersect at ($m\Omega$,K) = (0.138062,0.759145). For parameters above the dashed line an ergoregion exists at the equator.

Figure Ten. Restrictions for a/m = 0.5. The values of the parameters are restricted to the area bounded on the left by

the η inequality and the integral inequality (upper right) and the Boyer equatorial condition (lower right) which intersect at $(m\Omega,K) = (0.171489,0.829032)$. For parameters above the dashed line an ergoregion exists at the equator.

Figure Eleven. Restrictions for $a/m = 0.7$. The values of the parameters are restricted to an area bounded on the left by the η inequality and the integral inequality (upper right) and the Boyer equatorial condition (lower right) which intersect at $(m\Omega,K) = (0.222366,0.902967)$. For parameters above the dashed line an ergoregion exists at the equator. Note that the importance of the integral inequality is diminishing.

Figure Twelve. Restrictions for $a/m = 0.9$. The values of the parameters are restricted to an area bound on the left by the η inequality and the integral inequality (upper right) and the Boyer equatorial condition (lower right) which intersect at $(m\Omega,K) = 0.317761,0.973308)$. For parameters above the dashed line an ergoregion exists at the equator. Note that the importance of the integral inequality is diminishing rapidly as a/m increases.

Figure Thirteen. Restrictions for $a/m = 1$. In this limit the integral inequality imposes no restrictions. The restrictions come from the η inequality (upper curve) and the Boyer equatorial condition (lower curve) which intersect at $(m\Omega,K) = (0.5,1.0)$. Again for parameters above the dashed line an ergoregion exists at the equator.

Figure Fourteen. Restrictions for a/m = 1.01. The only restrictions come from the η inequality (upper curve) and the Boyer equatorial condition (lower curve) which intersect at (mΩ,K) = (0.333349,0.947707). For cases where a > m no ergoregions form.

Figure Fifteen. Restrictions for a/m = 1.5. The only restrictions come from the η inequality (upper cuvre) and the Boyer equatorial condition (lower curve) which intersect at (mΩ,K) = (0.134374,0.623607).

Figure Sixteen. Restrictions for a/m = 3.0. The only restrictions come from the η inequality (upper curve) and the Boyer equatorial condition (lower curve) which intersect at (mΩ,K) = (0.440216×10^{-1},0.327098).

Figure Seventeen. Restrictions for a/m = 5.23094. The restrictions for this case come from the η inequality (upper solid curve) and the Boyer equatorial condition (lower solid curve) which intersect at (mΩ,K) = (0.18273×10^{-1},0.19117). However, at this value of a/m the Boyer polar condition (dashed cuvre) begins to restrict the parameter range.

Figure Eighteen. Restrictions for a/m = 8. Restrictions come from the η inequality (at left), the Boyer equatorial condition (at right) and the Boyer polar condition (at top). The η inequality and the Boyer polar condition intersect at (mΩ,K) = (0.781211×10^{-2},0.125). The two Boyer conditions intersect at (mΩ,K) = (0.92748×10^{-2},0.125).

Figure Nineteen. Restrictions for a/m = 10. Restrictions come from the η inequality (at left) and the two Boyer conditions. The Boyer polar condition intersects the η inequality at $(m\Omega,K) = (0.5\times10^{-2},0.1)$. The two Boyer conditions intersect at $(m\Omega,K) = (0.652505\times10^{-2},0.1)$.

Figure Twenty. Restrictions for $a/m = 10^2$. Restrictions come from the η inequality (at left) and the two Boyer conditions. The Boyer polar condition intersects the η inequality at $(m\Omega,K) = (0.5\times10^{-4},10^{-2})$. The two Boyer conditions intersect at $(m\Omega,K) = (0.189298\times10^{-3},10^{-2})$. The importance of the η inequality is diminishing as a/m becomes larger.

Figure Twenty-one. Restrictions for $a/m = 10^3$. At this large value of a/m the restrictions demand that the configuration take on a slowly rotating ($\Omega<<1$) and a nearly Newtonian ($K<<1$) form. In this Newtonian regime the effect of the η inequality begins to be negligible.

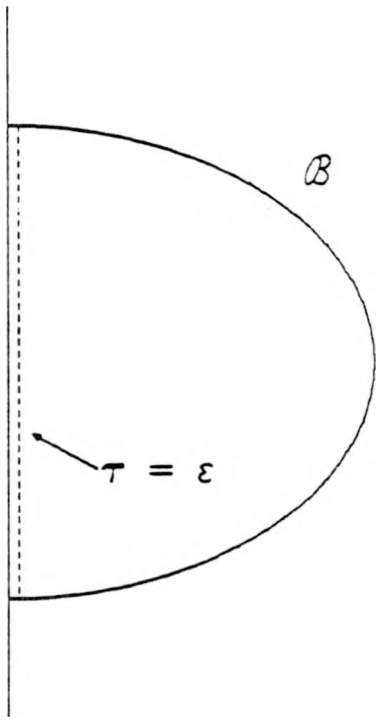

Figure One.

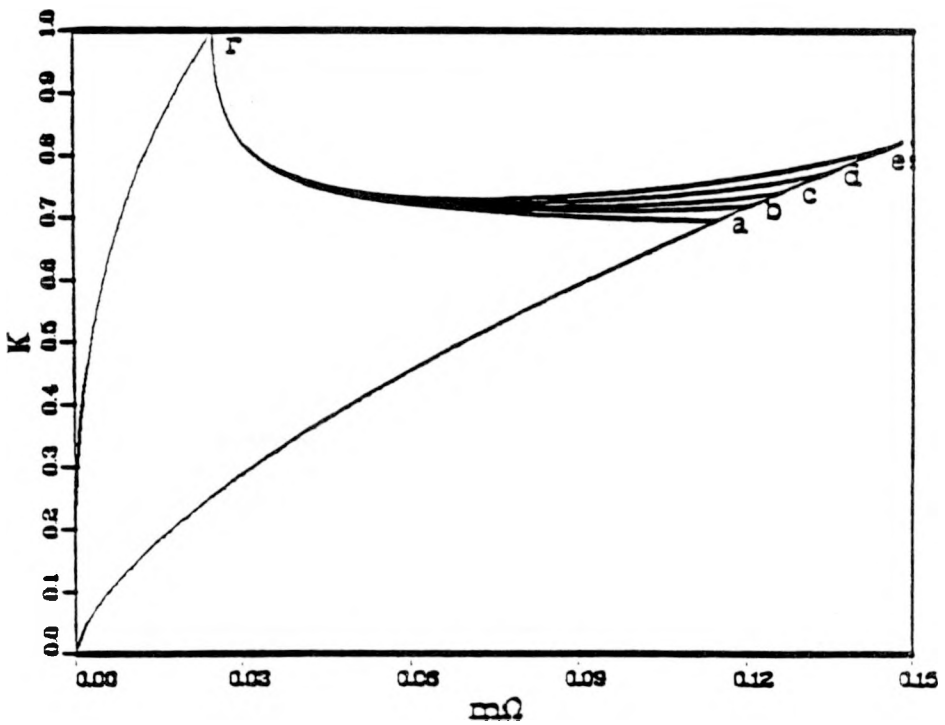

Figure Two.

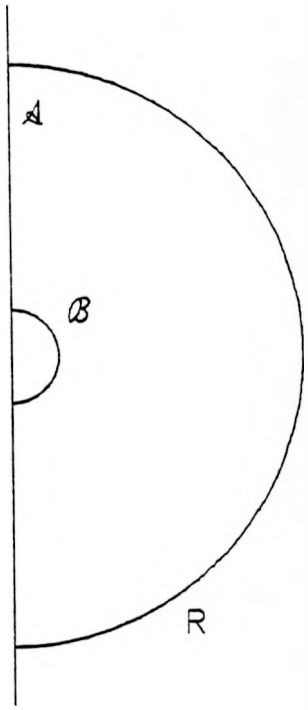

Figure Three.

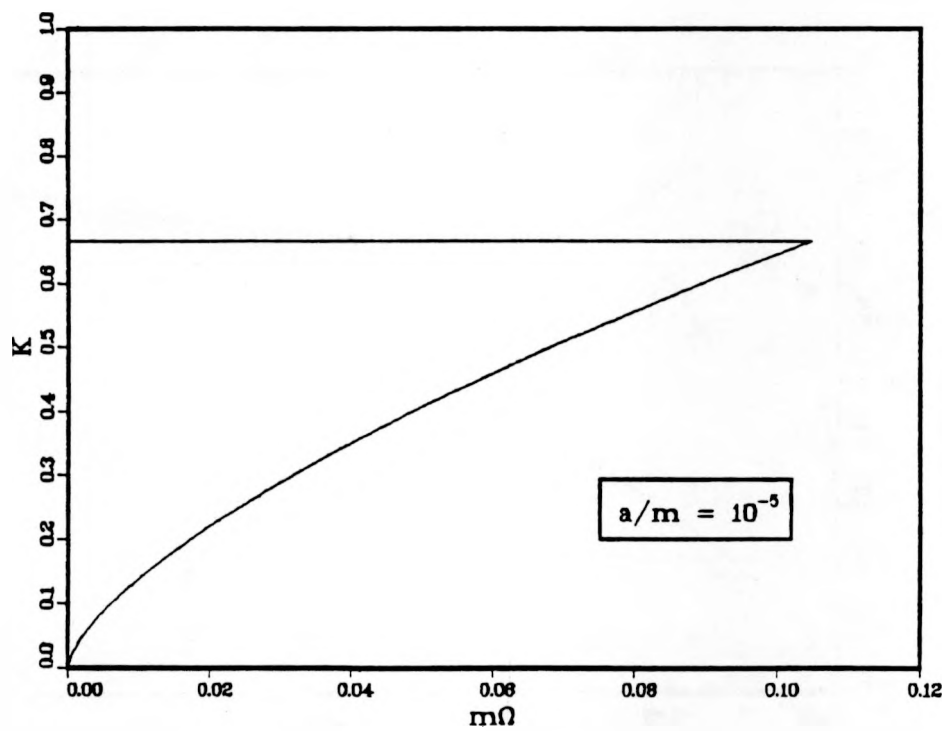

Figure Four.

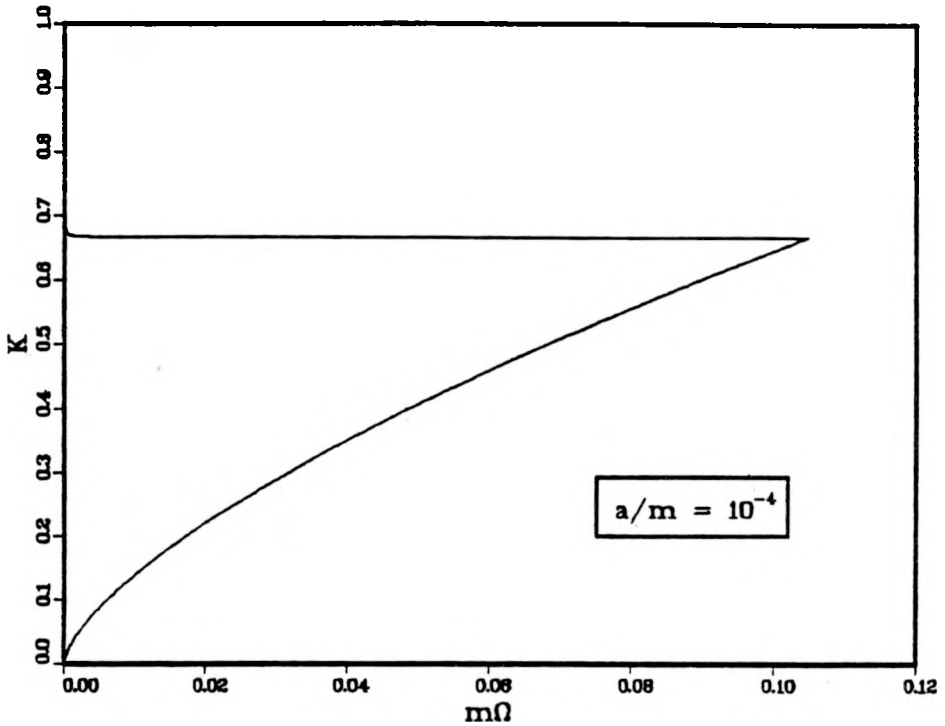

Figure Five.

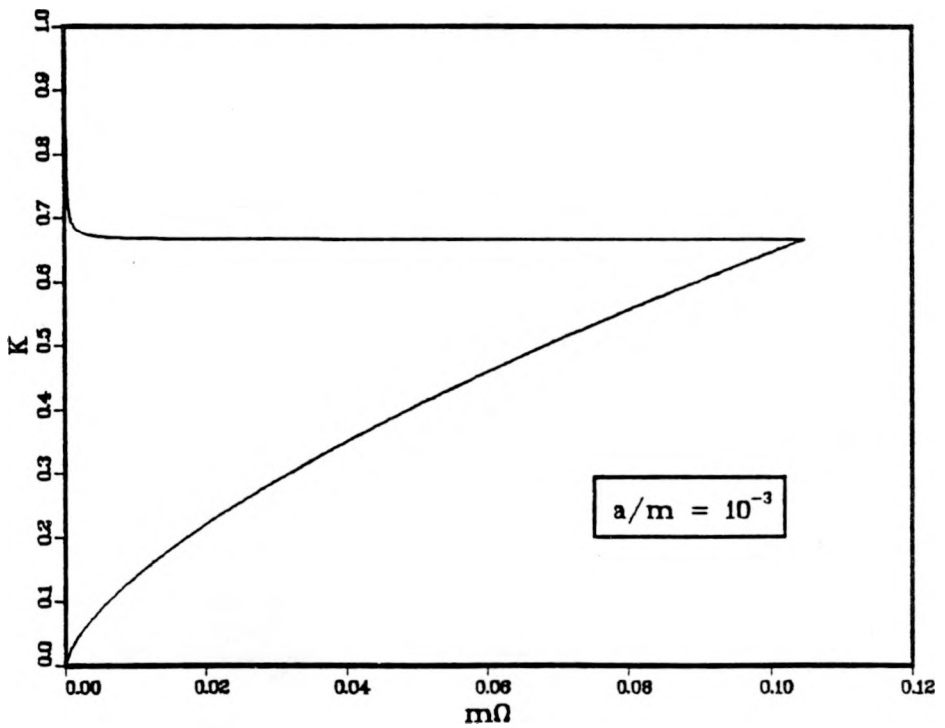

Figure Six.

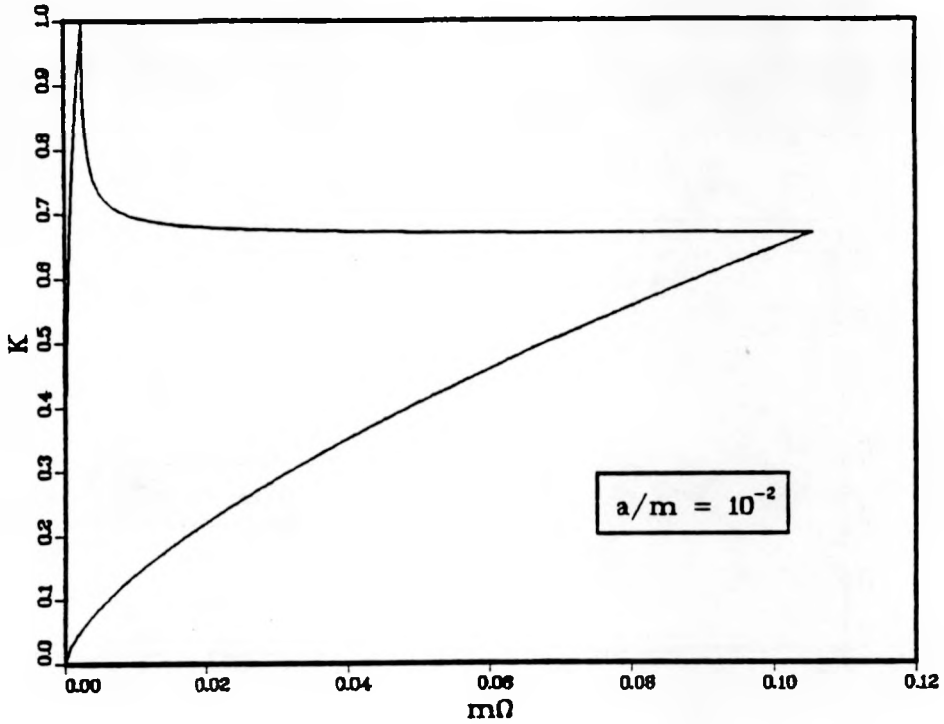

Figure Seven.

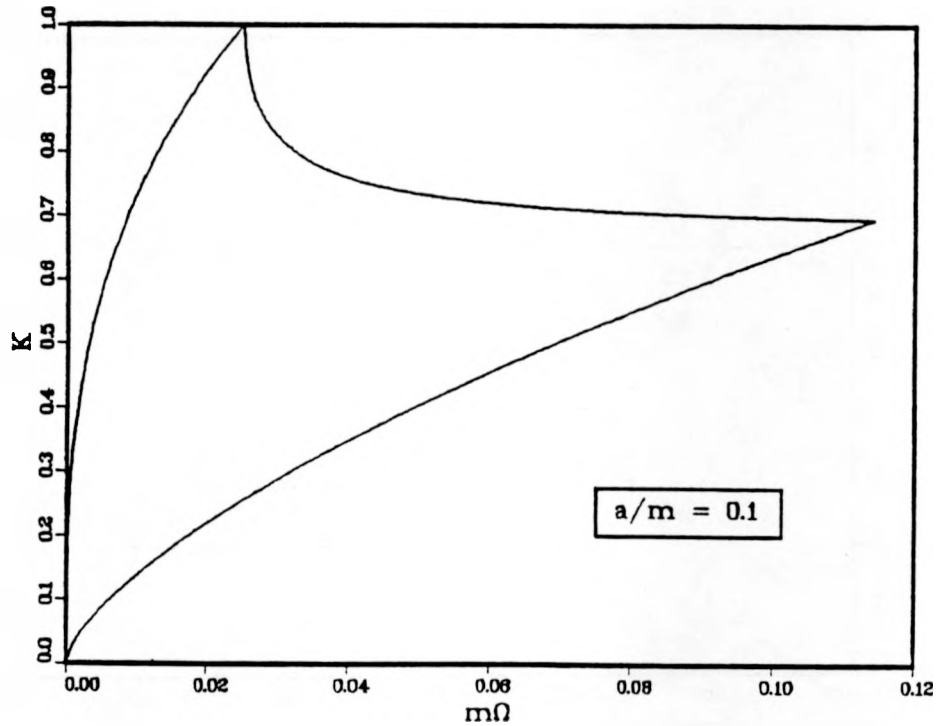

Figure Eight.

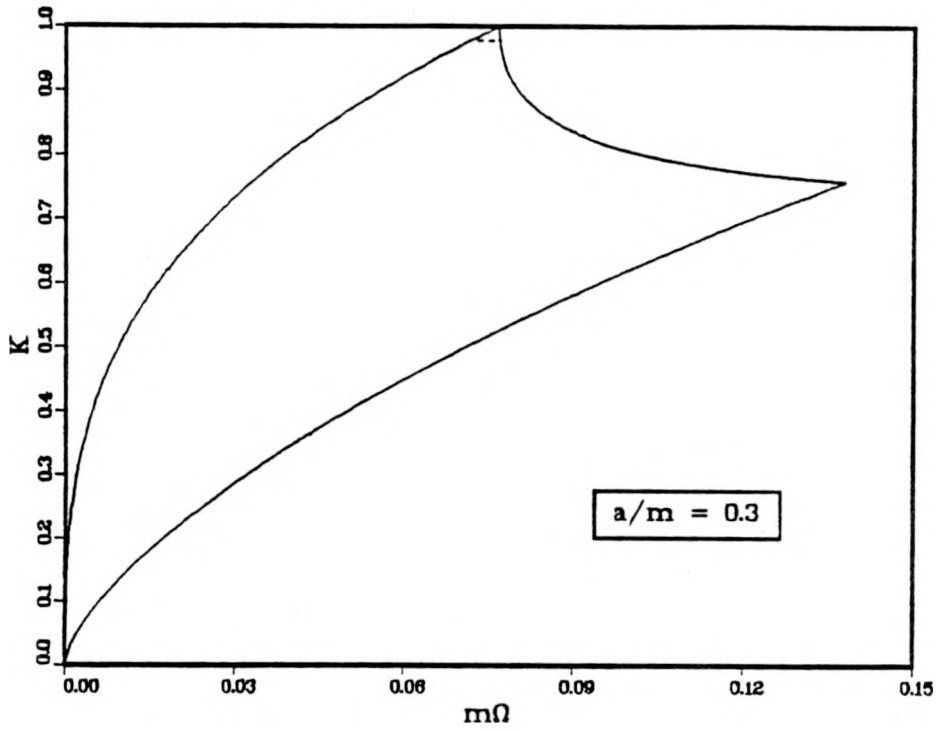

Figure Nine.

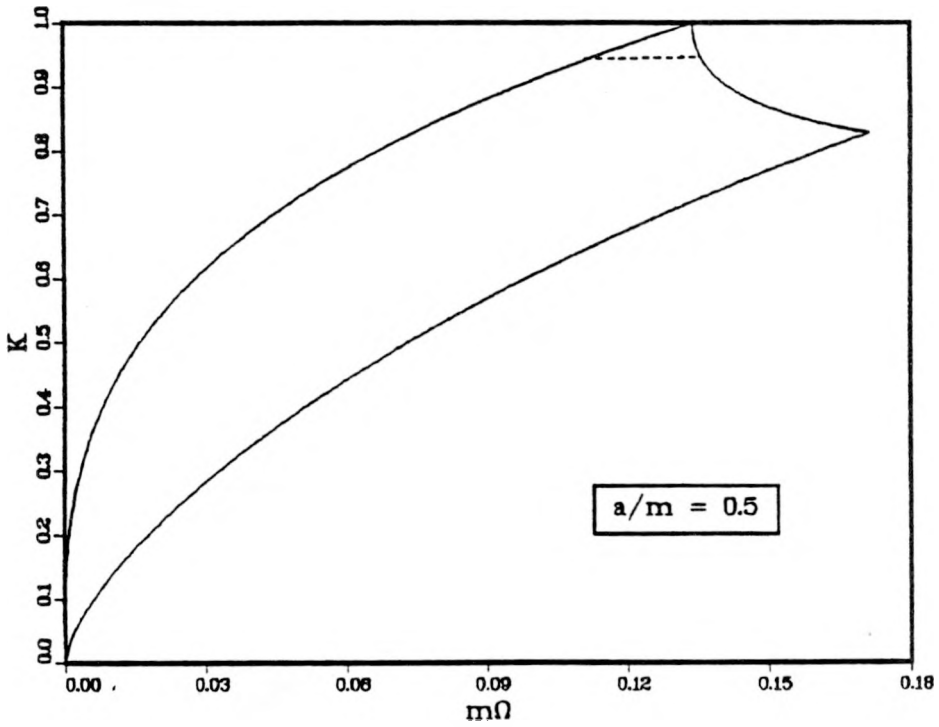

Figure Ten.

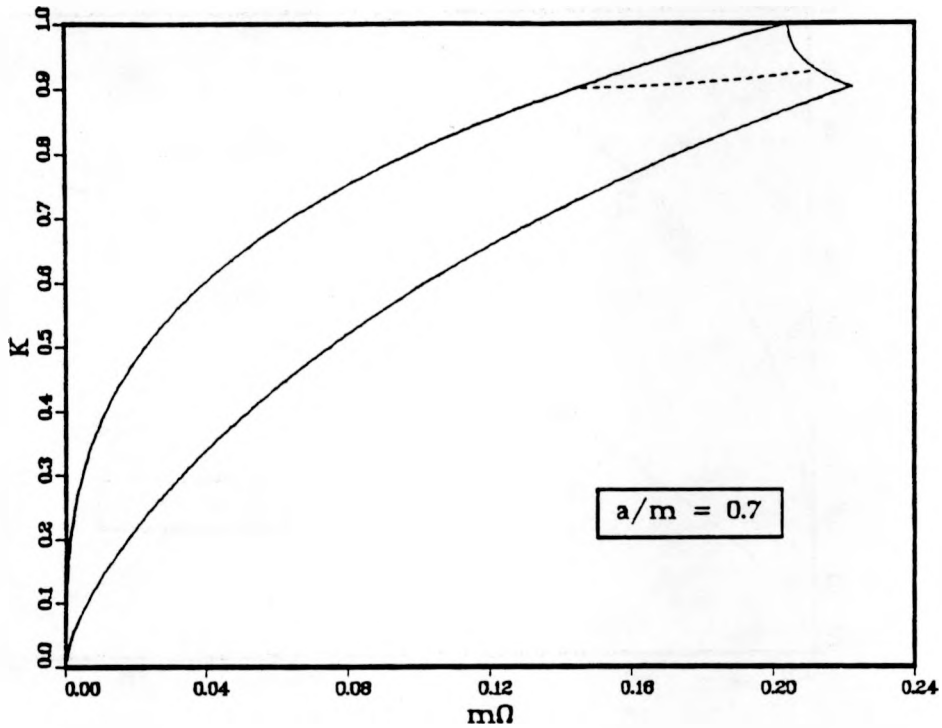

Figure Eleven.

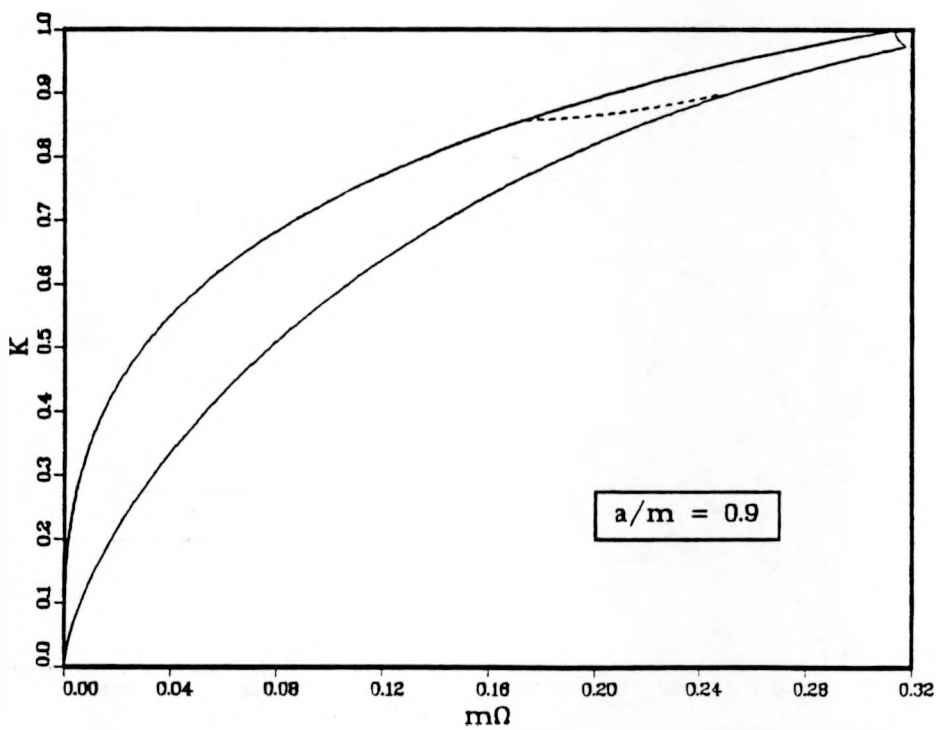

Figure Twelve.

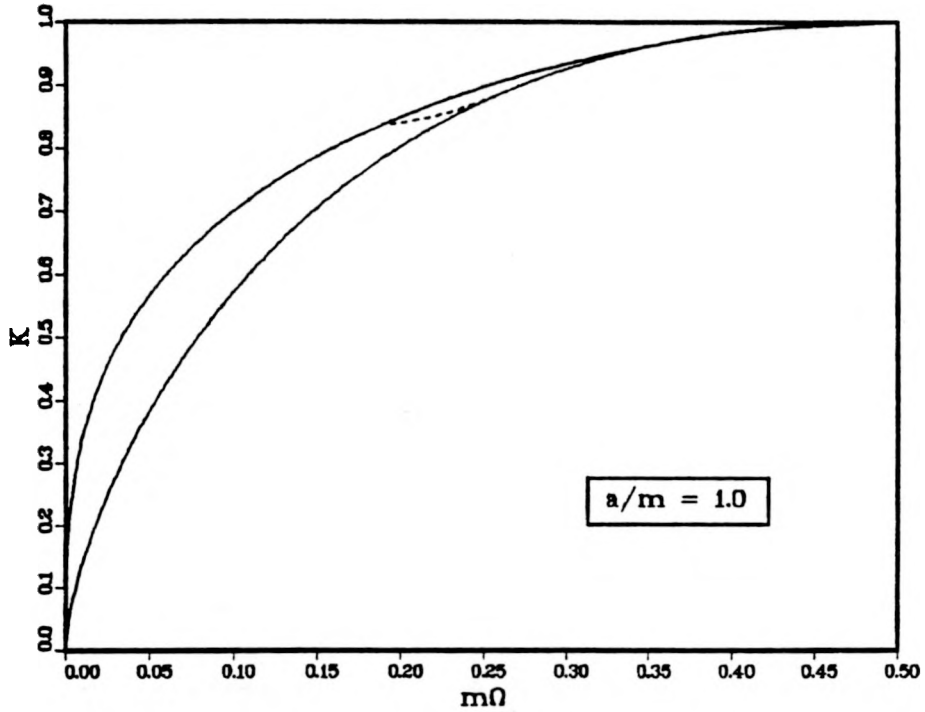

Figure Thirteen.

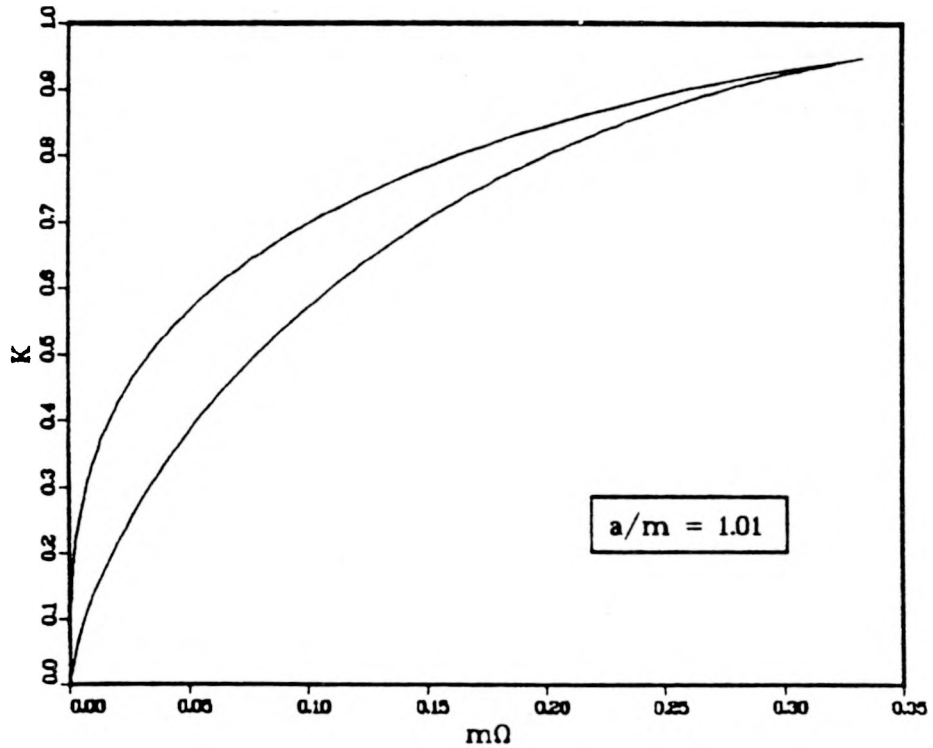

Figure Fourteen.

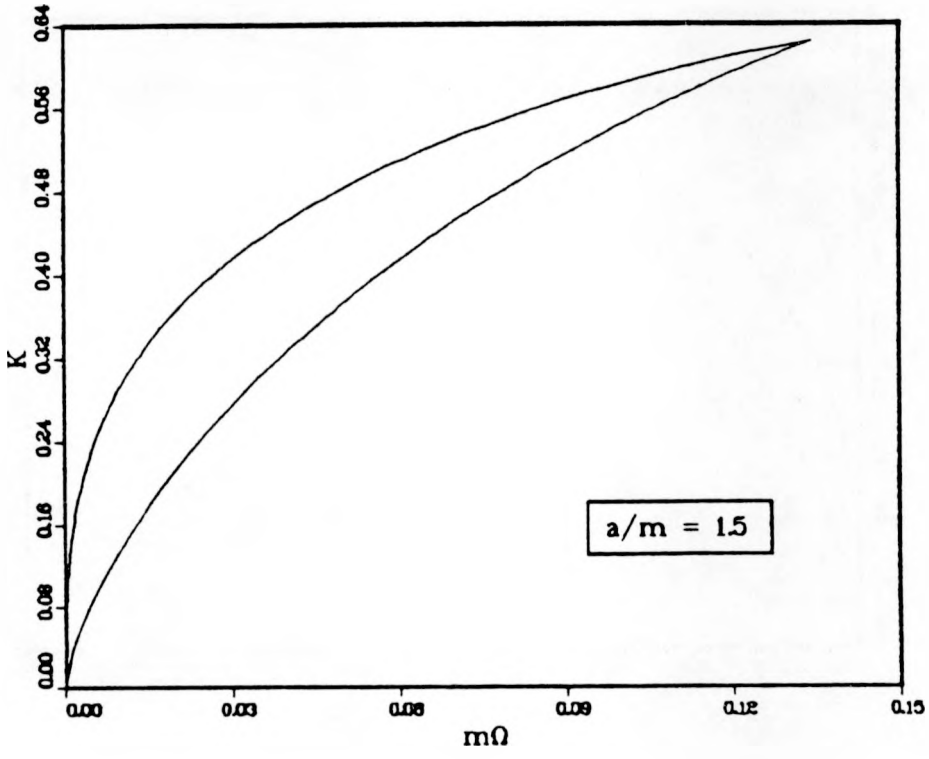

Figure Fifteen.

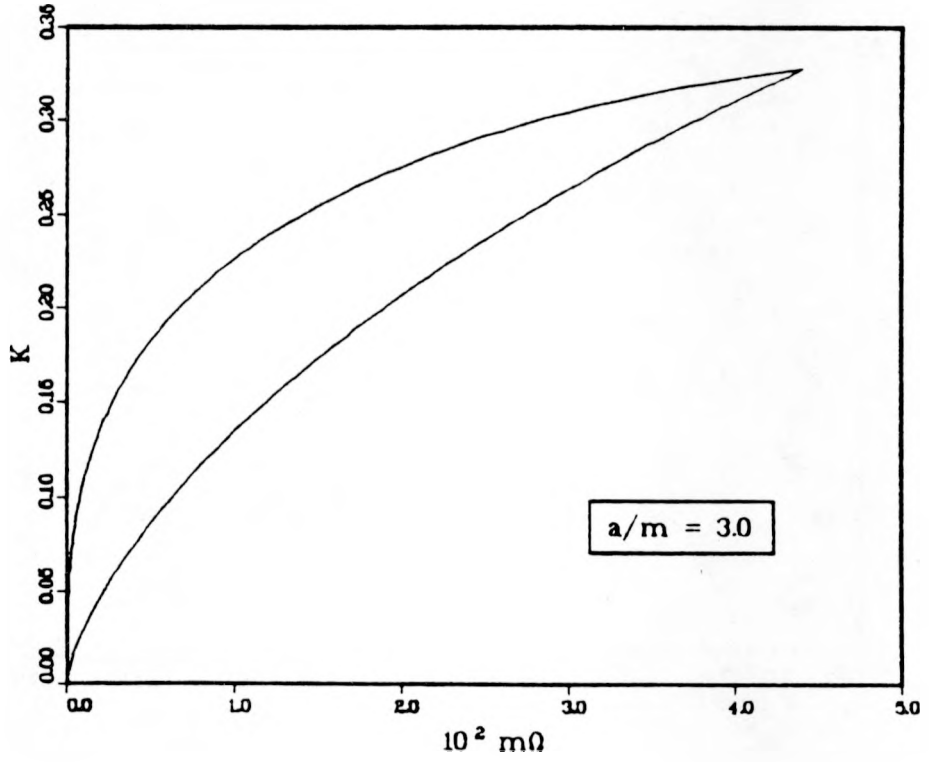

Figure Sixteen.

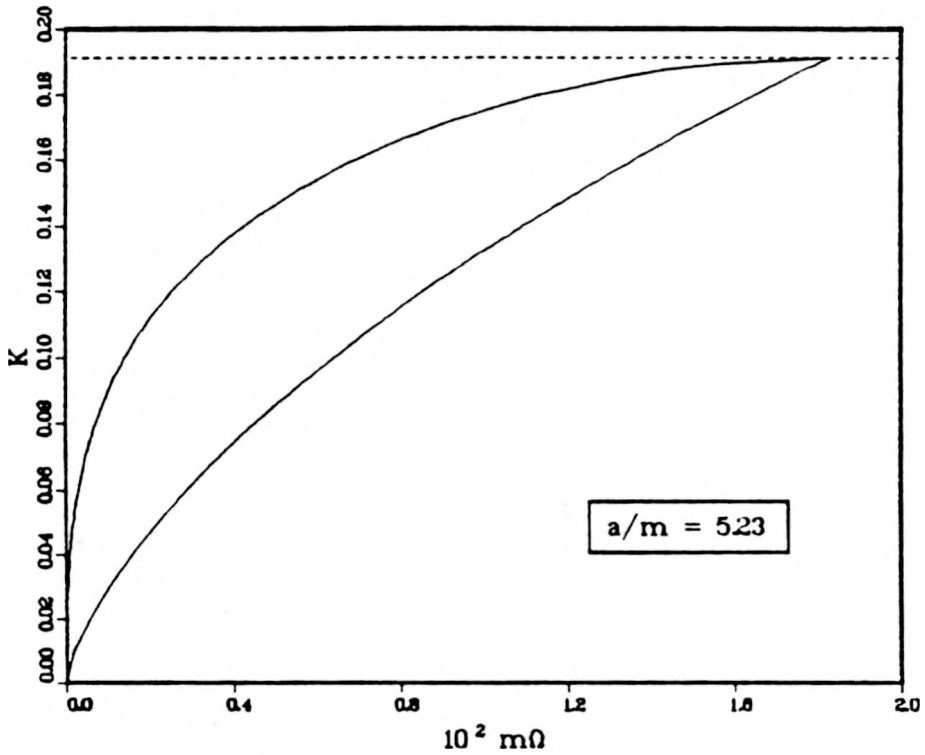

Figure Seventeen.

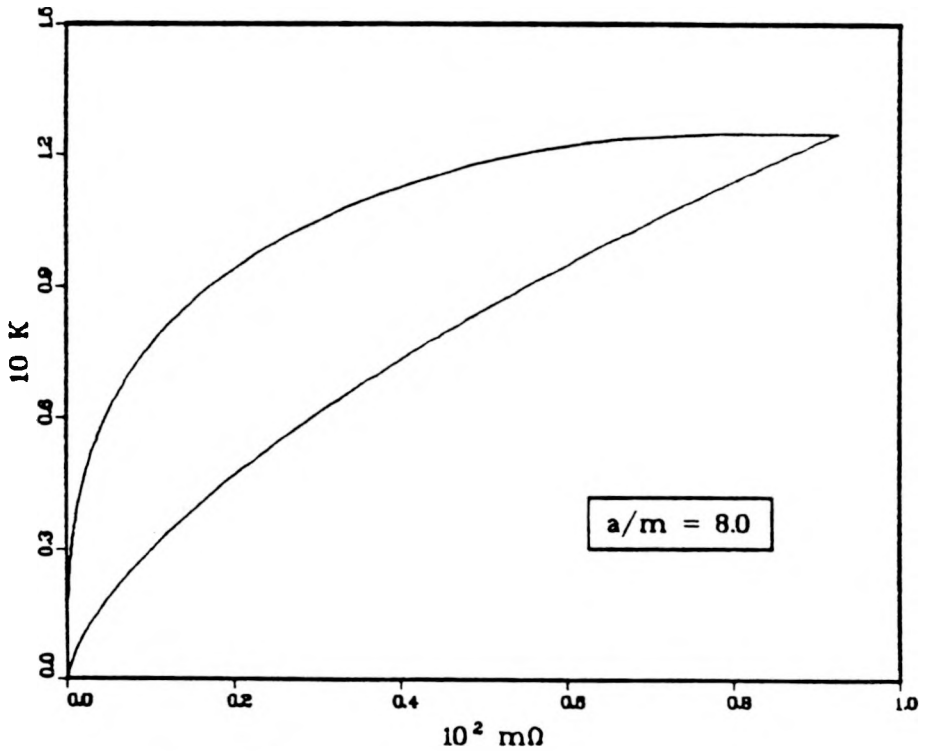

Figure Eighteen.

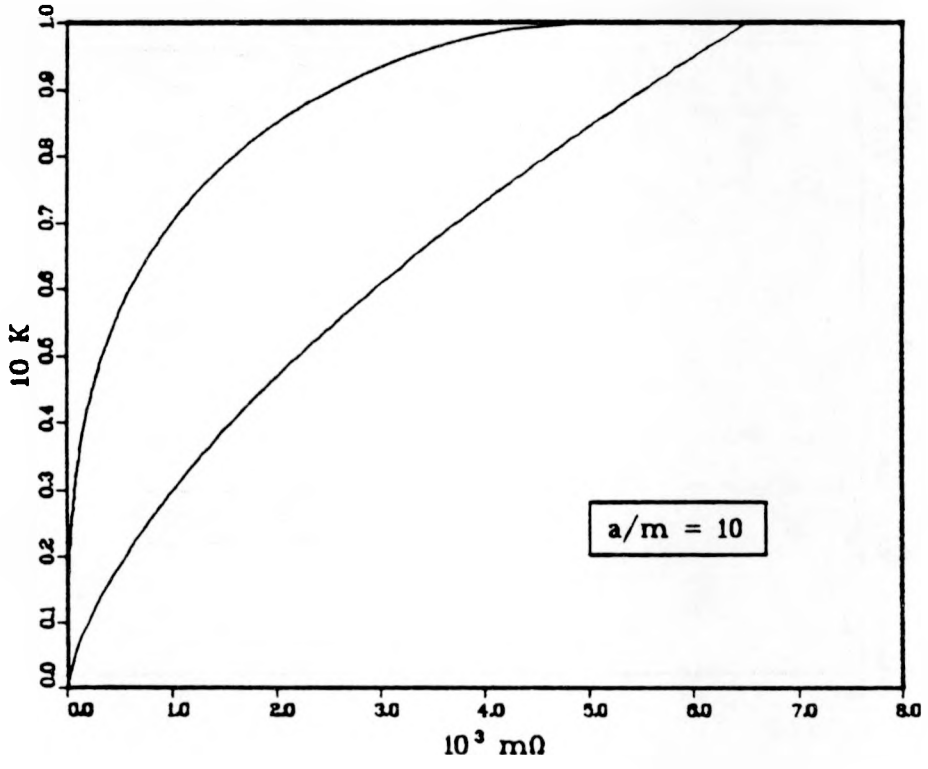

Figure Nineteen.

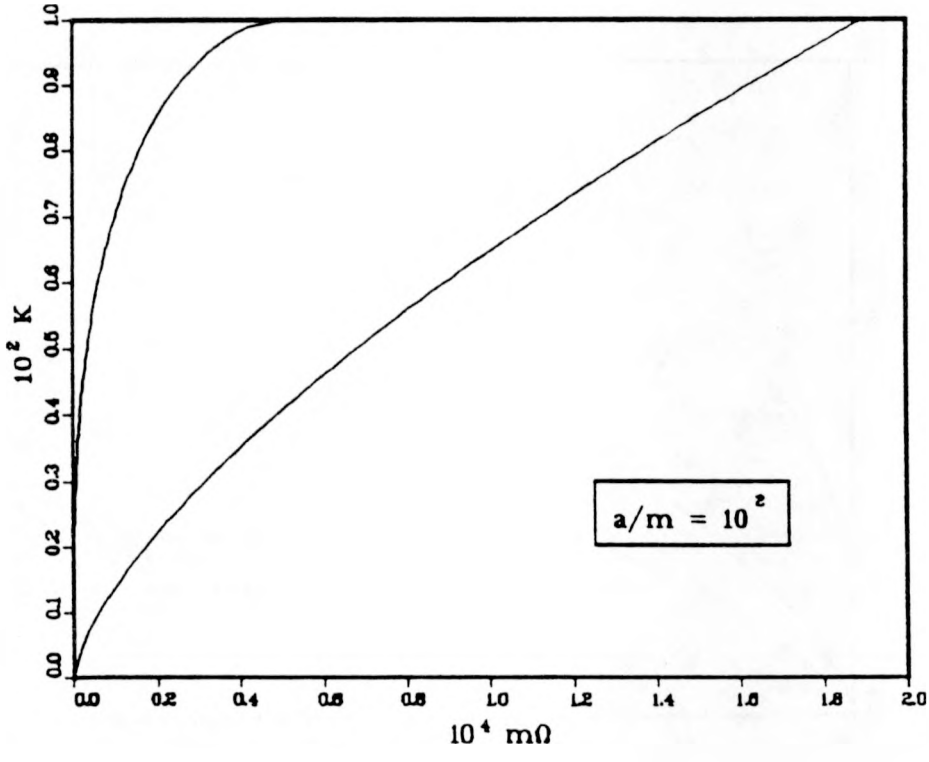

Figure Twenty.

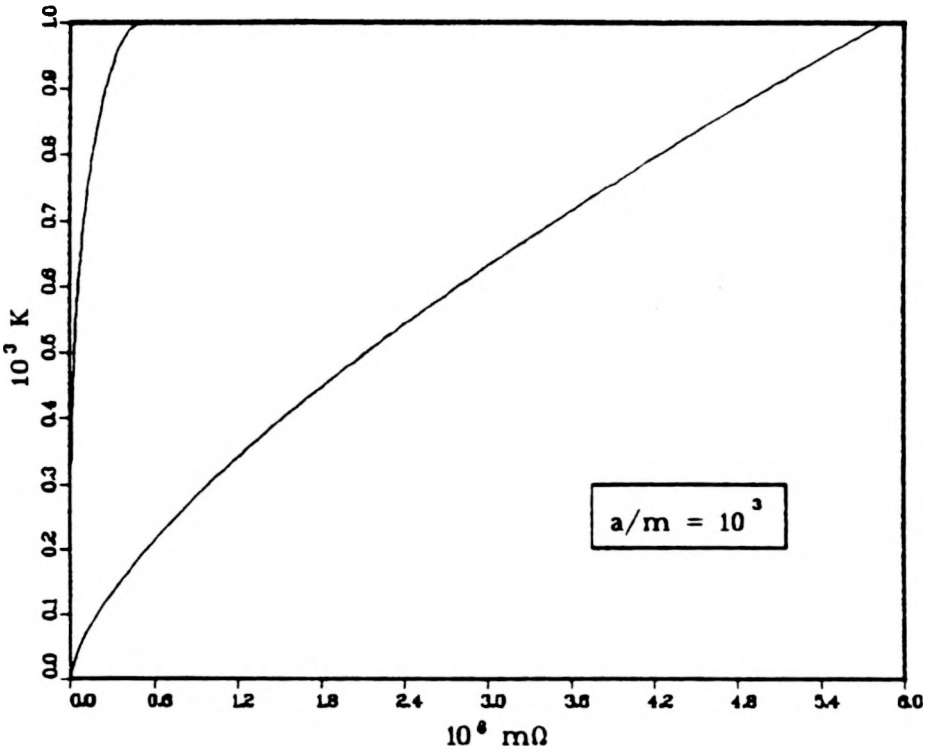

Figure Twenty–one.

☆ U. S. GOVERNMENT PRINTING OFFICE 1981-0-777-022/50